Aerosol Physics

ENV-409

Diverse and complex characteristics of particulate matter (aerosols)

- PM size, morphology, and composition varies in time and space
  - Difficult to characterize comprehensively
  - Measurement artifacts:
    - collection efficiencies (size or composition-dependent)
    - chemical and physical transformations can occur between collection and analysis
- *What is the PM concentration?*
  - The answer will likely depend on what device you use to measure it
- *How to design a device for particle capture?*
  - measurement and PM emissions control
- *How do you model ultimate fate and impact of PM?*
  - Depends on which impact you want to consider

Contents

- Descriptions of aerosol size distributions
- Applications of aerosol physics
  - sampling and measurement
  - air pollution control
  - respiratory health
- Theory of aerosol physics (single particle description)

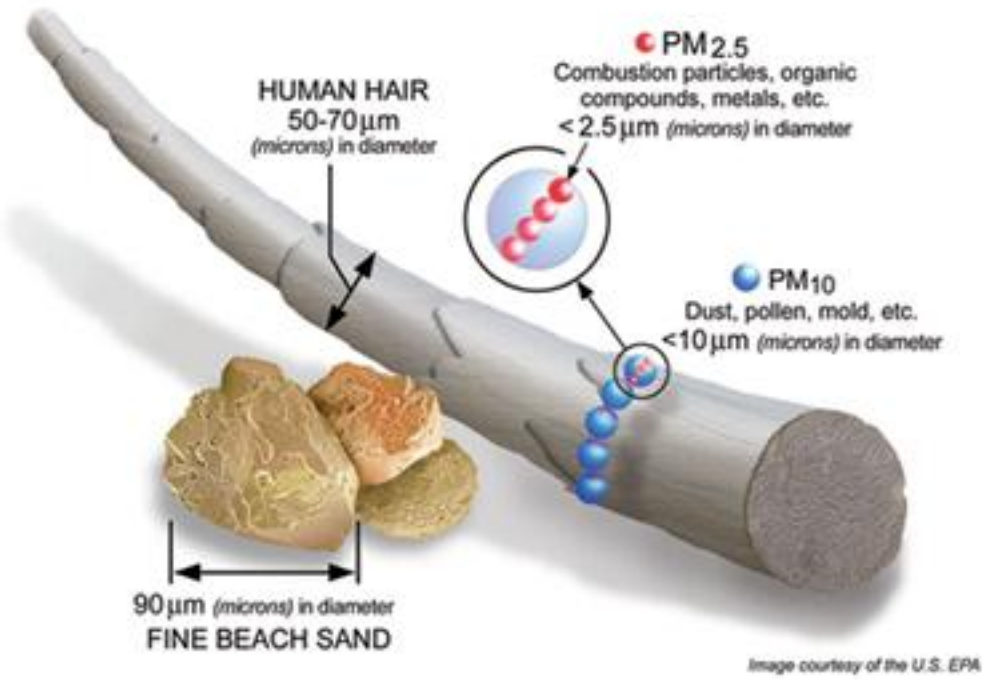

Metrics of aerosol size

Geometric diameter

$$D_{geom}$$

Stokes diameter

$$D_{Stk} = \left(\frac{18 v_s \mu}{\rho_p g C_c(D_{Stk})} \right)^{1/2}$$

Volume-equivalent diameter

$$D_{ve} = \frac{6}{\pi} V_p^{1/3}$$

Electrical mobility diameter

$$D_{em} = D_{ve} \chi \frac{C_c(D_{em})}{C_c(D_{ve})}$$

Classical aerodynamic diameter

$$D_{\mathrm{ca}} = \left(\frac{18 v_s \mu}{\rho_p^\circ g C_c(D_{\mathrm{ca}})} \right)^{1/2} = D_{ve} \left(\frac{\rho_p}{\rho_p^\circ \chi} \frac{C_c(D_{ve})}{C_c(D_{ca})} \right)^{1/2}$$

Vacuum aerodynamic diameter

$$D_{va} \approx D_{ve} \frac{\rho_p}{\rho_p^\circ \chi}$$

In the continuum regime ($2\lambda \gg D_p$), slip correction $C_c \sim 1$

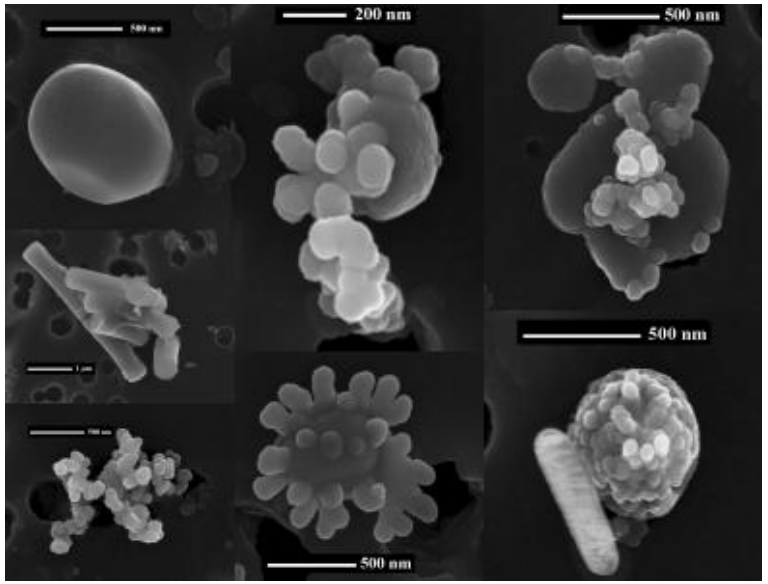

Coz et al., *Aerosol Sci. Tech.*, 2008

Dynamic shape factor

$$\chi = \frac{F_D}{F_D^{\mathrm{ve}}}$$

Shape factor

$$\chi = \phi\left(\mathrm{shape}, Kn(D_p)\right) \chi^{(\mathrm{shape})}$$

Metrics of aerosol size

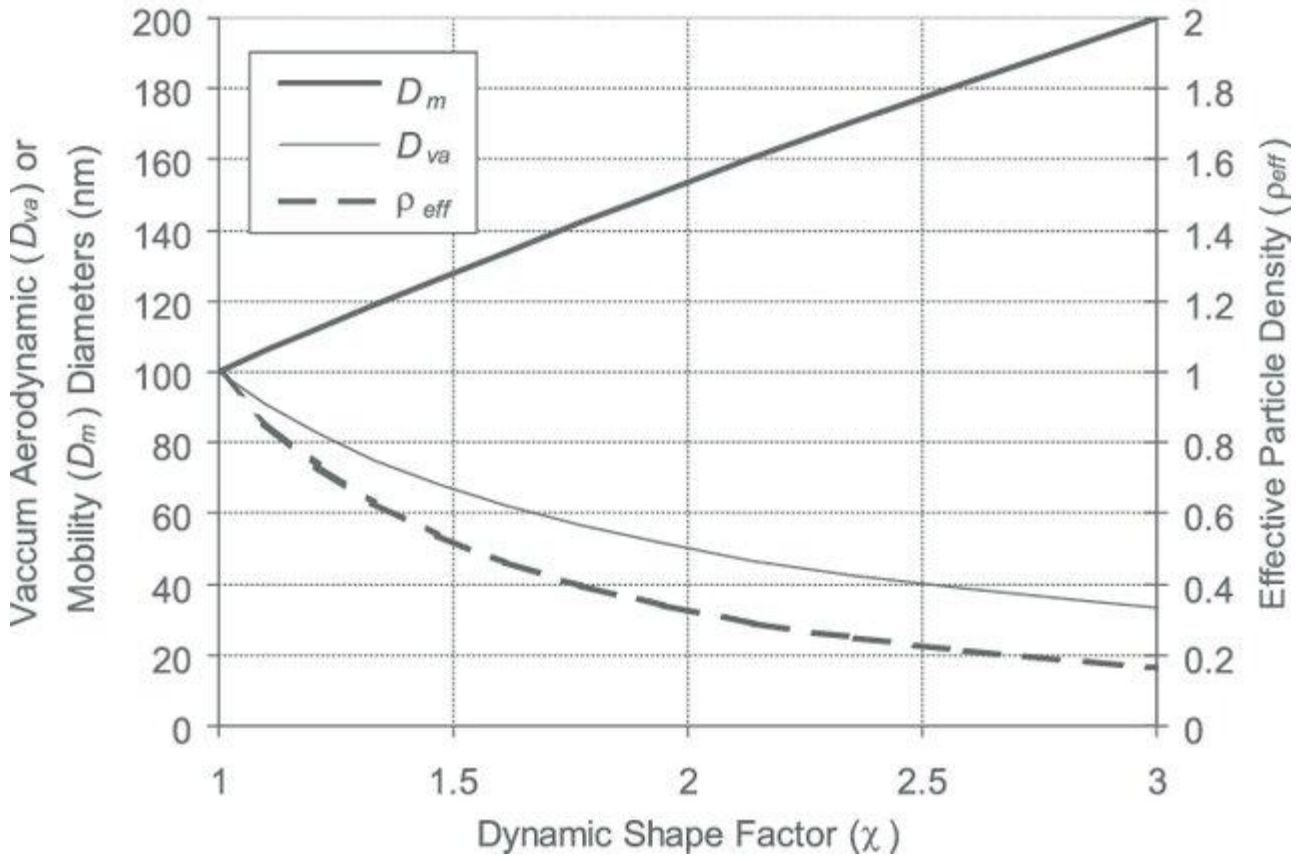

Shape	Dynamic shape factor
Sphere	1.00
Cube	1.08
Cylinder (L/D = 2); horizontal axis	1.14
Cylinder (L/D = 2); vertical axis	1.01
Straight chain (L/D = 2)	1.10
Sand	1.57
Talc	1.88

L = length and D = diameter

Mn et al., *Food Rev. Int.*, 2021

Figure 9. Calculated variation of the mobility diameter, vacuum aerodynamic diameter, and effective density (D_{va}/D_m) for a particle with a volume equivalent diameter (D_v) of 100 nm as a function of the dynamic shape factor χ (assuming $\chi = \chi_v$) for particles of unit material density (ρ_p = 1 g cm^{-3}).

Jimenez et al., *J. Geophys. Res.*, 2003

In this lecture

- Understand how to interpret number size distributions (relevant for colloidal suspensions in other domains)
  - normalize to view an unbiased representation.
- Describe the motion of individual particles by a force balance.
- Categorize different types of “artifacts” (errors which are introduced by the instrument or analytical technique during sampling and measurement)
- Explain challenges for sample collection and particulate matter removal from effluent streams.
- Calculate fate of particles in an airstream.

Number size distributions

TABLE 8.1 Example of Segregated Aerosol Size Information

Size Range, μm	Concentration, cm^{-3}	Cumulative, cm^{-3}	Concentration, $\mu m^{-1}\ cm^{-3}$
0.001–0.01	100	100	11,111
0.01–0.02	200	300	20,000
0.02–0.03	30	330	3,000
0.03–0.04	20	350	2,000
0.04–0.08	40	390	1,000
0.08–0.16	60	450	750
0.16–0.32	200	650	1,250
0.32–0.64	180	830	563
0.64–1.25	60	890	98
1.25–2.5	20	910	16
2.5–5.0	5	915	2
5.0–10.0	1	916	0.2

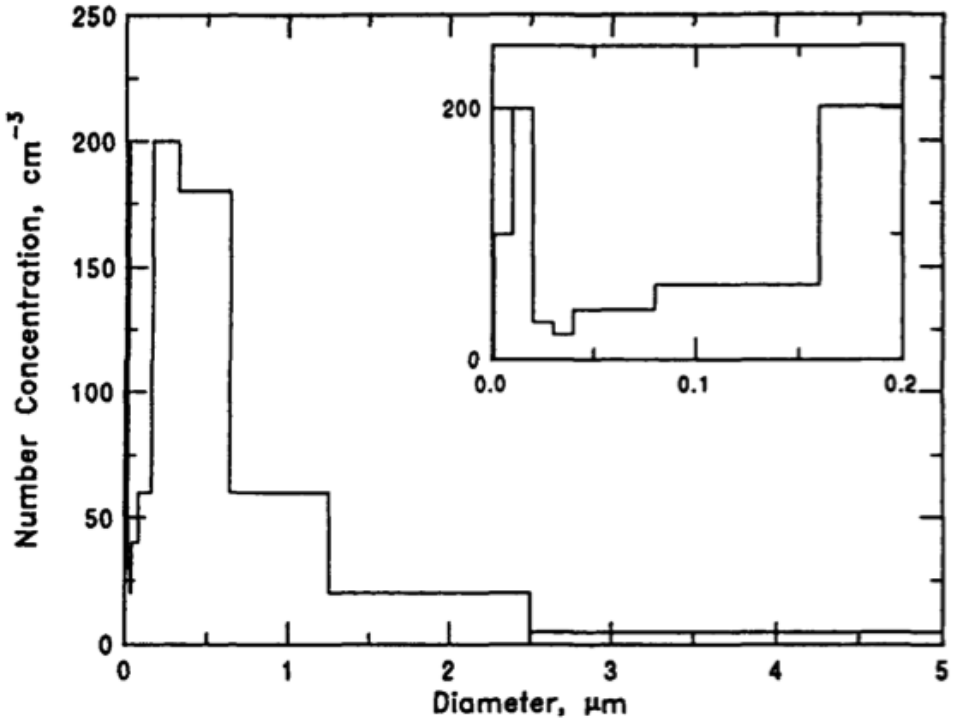

FIGURE 8.1 Histogram of aerosol particle number concentrations versus the size range for the distribution of Table 8.1. The diameter range 0–0.2 μm for the same distribution is shown in the inset.

Normalizing the aerosol size distribution

Aerosol concentration in size interval i:

$$N_i = n_i \Delta D_{p,i}$$

Let all $\Delta D_{p,i} \rightarrow 0$ such that $dD_p = \Delta D_p = \Delta D_{p,i}$. Then,

$n_N(D_p)dD_p$ = number of particles per volume of air having diameters in the range D_p to $(D_p + dD_p)$

Typically, volume is expressed in cm^3 and D_p in μm (though nm is also used).

Total number of particles (units of cm^{-3}):

$$N_t = \int_0^\infty n_N(D_p)dD_p$$

Total number of particles smaller than D_p (units of cm^{-3}):

$$N(D_p) = \int_0^{D_p} n_N(D_p^*)dD_p^*$$

We can see that:

$$n_N(D_p) = dN/dD_p$$

Lognormal transformations of the size distribution

Because aerosol sizes can span several orders of magnitude, we generally express the number size distribution as functions of $\log D_p$ (logarithm of base 10) rather than D_p.

$$n_N(\log D_p) = dN/d\log D_p$$

Note that since we cannot take logarithms of a dimensional quantity, we imply normalization by a reference diameter:

$$\log D_p \equiv \log\left(D_p/1\ \mu\text{m}\right)$$

Then,

$n_N(\log D_p)d\log D_p$ = number of particles per volume of air having diameters in the range $\log D_p$ to $(\log D_p + d\log D_p)$

Normalized number size distributions

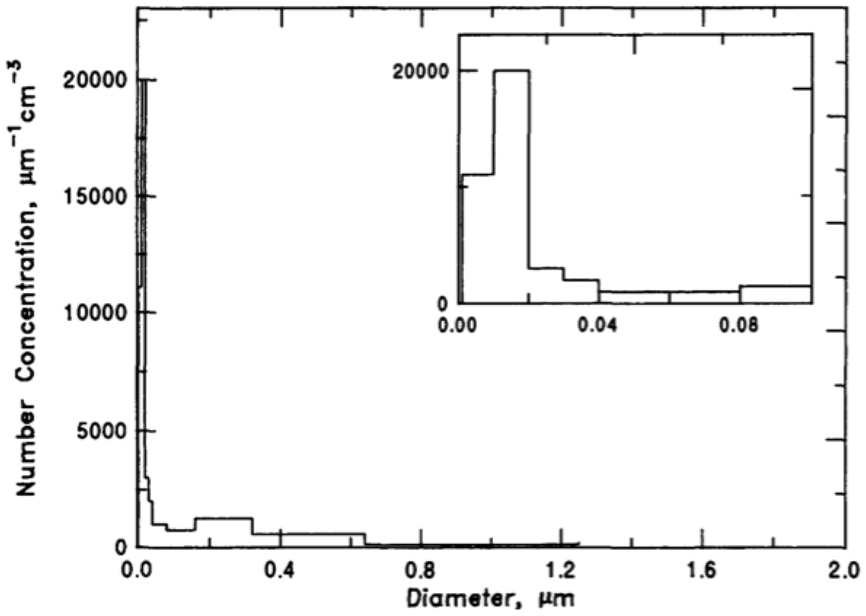

FIGURE 8.2 Aerosol number concentration normalized by the width of the size range versus size for the distribution of Table 8.1. The diameter range 0–0.1 μm for the same distribution is shown in the inset.

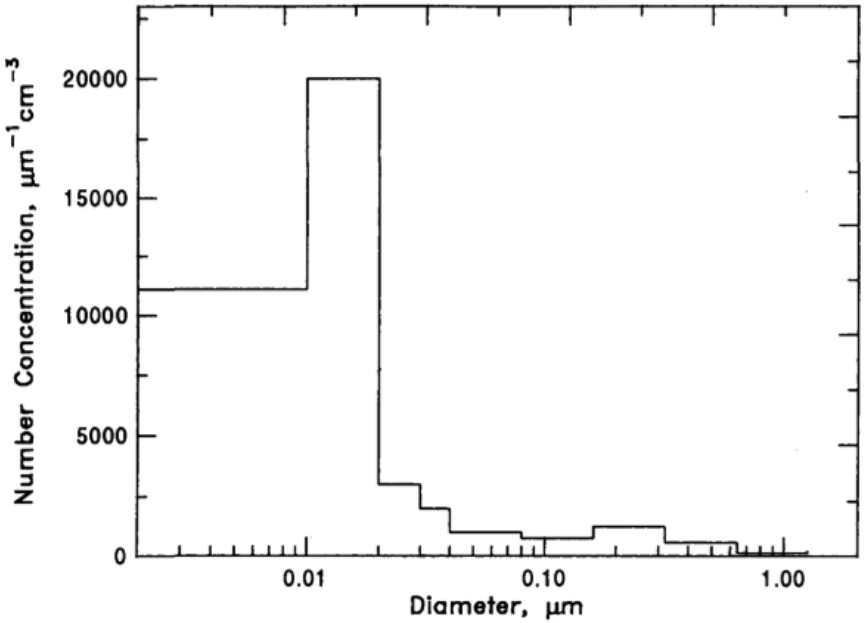

FIGURE 8.3 Same as Figure 8.2 but plotted against the logarithm of the diameter.

Moments of the aerosol size distribution

Moments of the size distribution, assuming spherical particles:

Zeroth (number): $$N_t = \int_{-\infty}^{\infty} \frac{dN}{d\log D_p} d\log D_p$$

Second (surface area): $$S_t = \pi \int_{-\infty}^{\infty} D_p^2 \frac{dN}{d\log D_p} d\log D_p$$

Third (volume): $$V_t = \frac{\pi}{6} \int_{-\infty}^{\infty} D_p^3 \frac{dN}{d\log D_p} d\log D_p$$

Mass is related to the volume by the size-dependent density $\rho(D_p)$, or size-weighted effective density $\bar{\rho}$:

$$M_t = \frac{\pi}{6} \int_{-\infty}^{\infty} \rho(D_p)\, D_p^3 \frac{dN}{d\log D_p} d\log D_p = \frac{\pi}{6} \bar{\rho} \int_{-\infty}^{\infty} D_p^3 \frac{dN}{d\log D_p} d\log D_p$$

Working with ensemble-averaged quantities

General relation:

$$\langle x^n \rangle = \frac{\int x^n f(x) dx}{\int f(x) dx}$$

Mean diameter:

$$\langle D_p \rangle_{\text{number}} = \left(\frac{\int D_p \frac{dN}{d \log D_p} d \log D_p}{\int \frac{dN}{d \log D_p} d \log D_p} \right)$$

Volume-equivalent diameter:

$$\langle D_p \rangle_{\text{volume}} = \left(\frac{\int D_p^3 \frac{dN}{d \log D_p} d \log D_p}{\int \frac{dN}{d \log D_p} d \log D_p} \right)^{1/3}$$

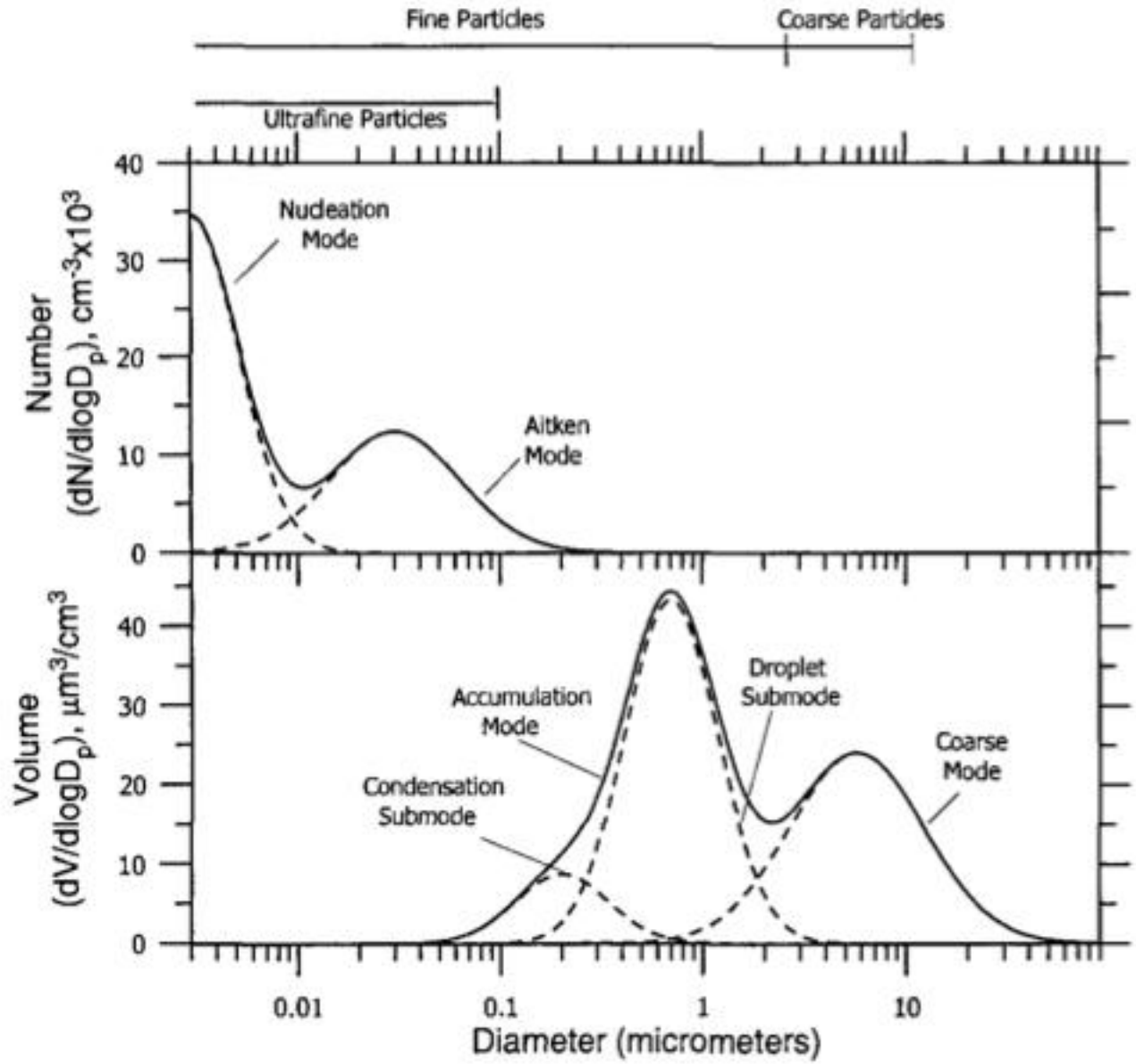

FIGURE 8.10 Typical number and volume distributions of atmospheric particles with the different modes.

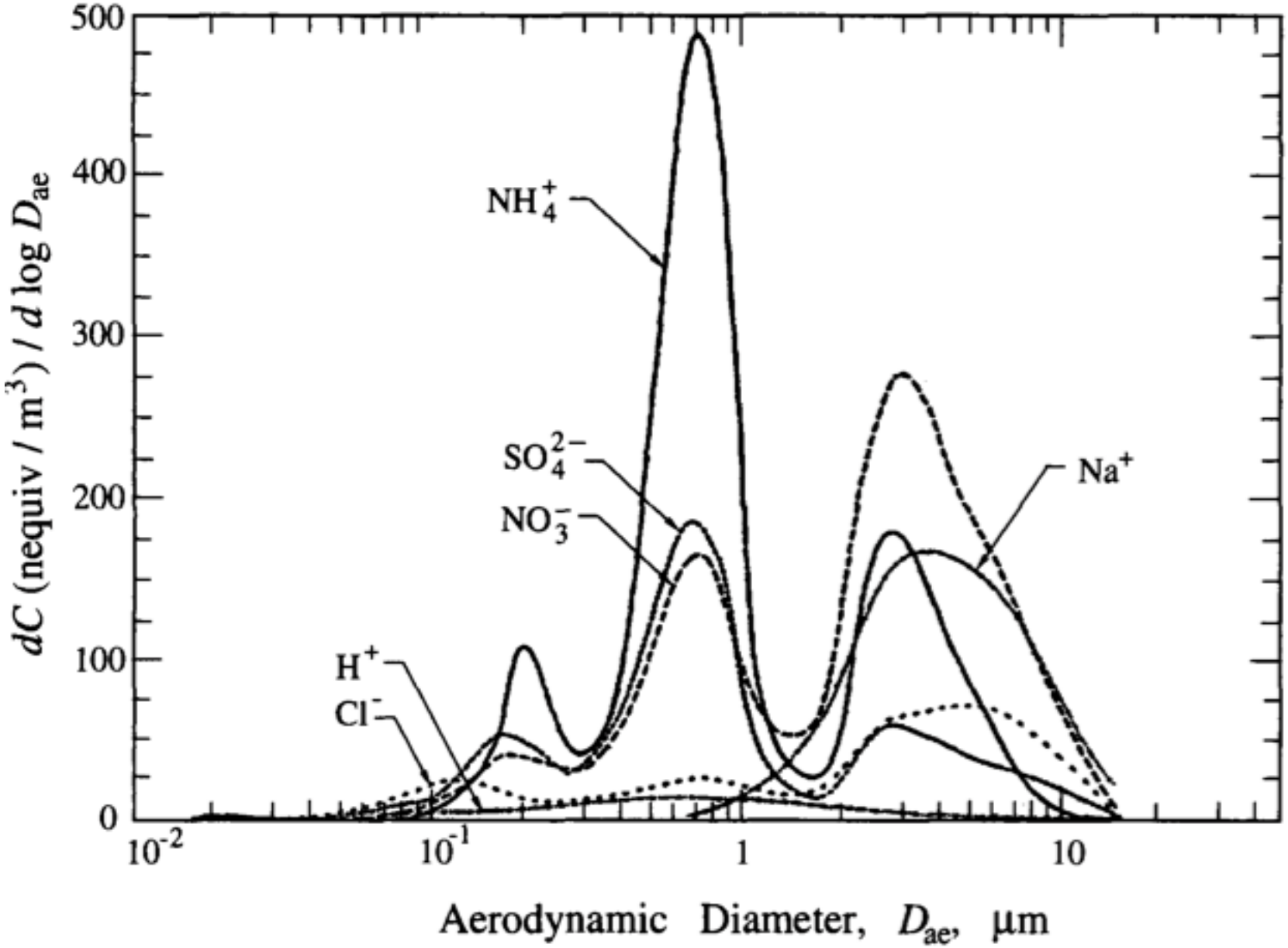

FIGURE 8.23 Measured size distributions of aerosol sulfate, nitrate, ammonium, chloride, sodium, and hydrogen ion in Claremont, CA (Wall et al. 1988).

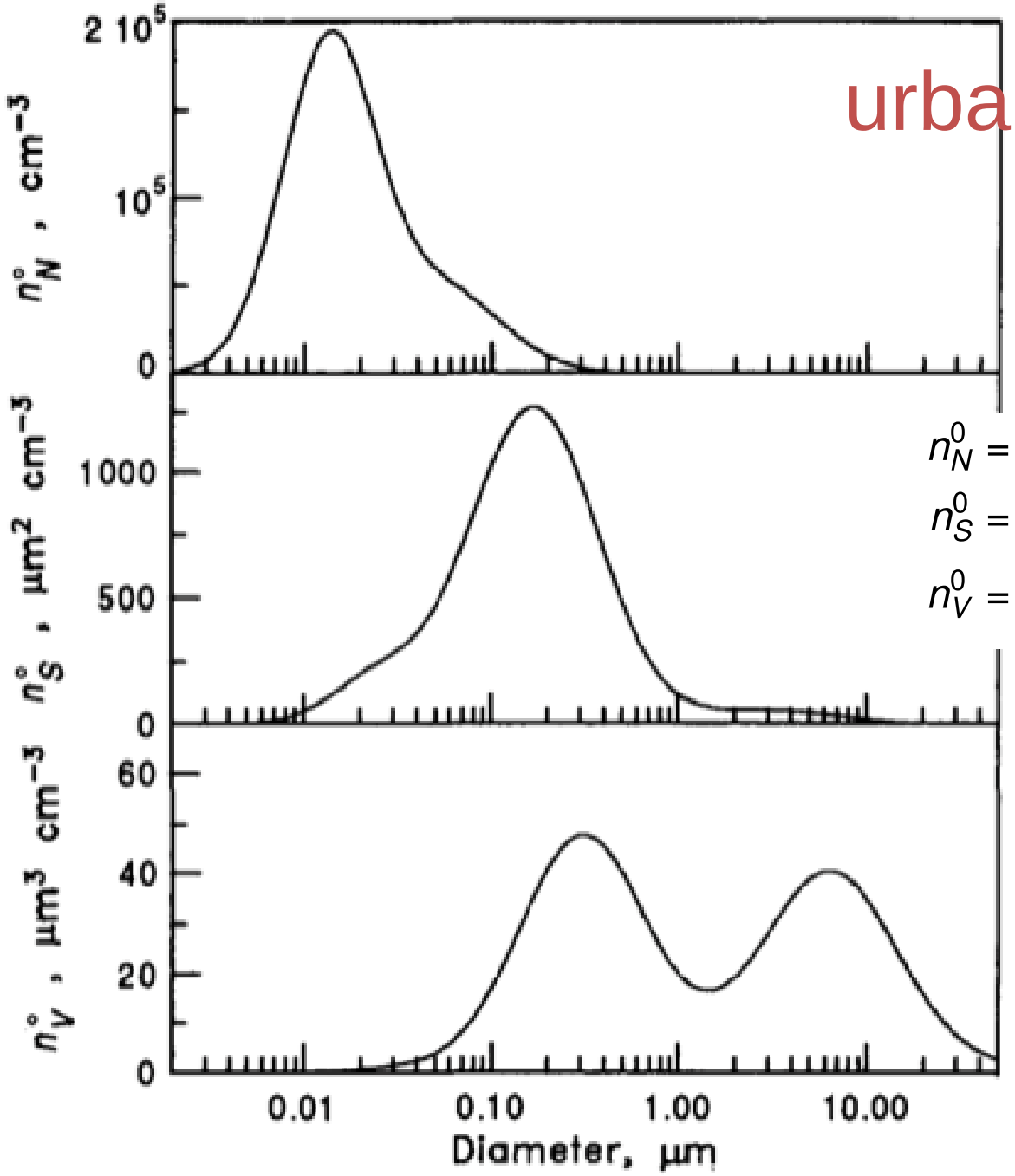

$$n_N^0 = n_N(\log D_p)$$

$$n_S^0 = \pi D_p^2 n_N(\log D_p)$$

$$n_V^0 = \frac{\pi}{6} D_p^3 n_N(\log D_p)$$

FIGURE 8.11 Typical urban aerosol number, surface, and volume distributions.

rural
continental

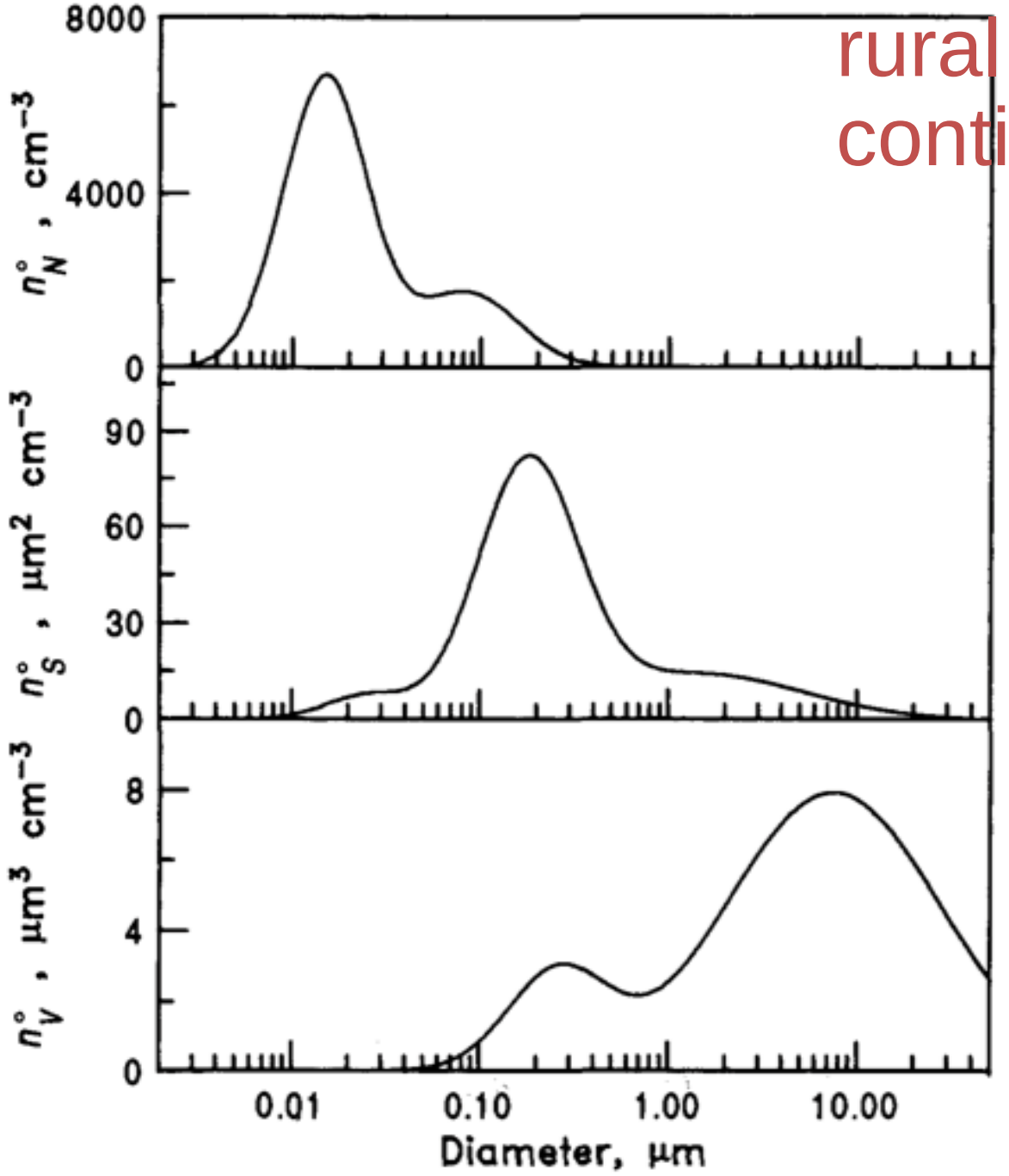

FIGURE 8.17 Typical rural continental aerosol number, surface, and volume distributions.

remote
continental

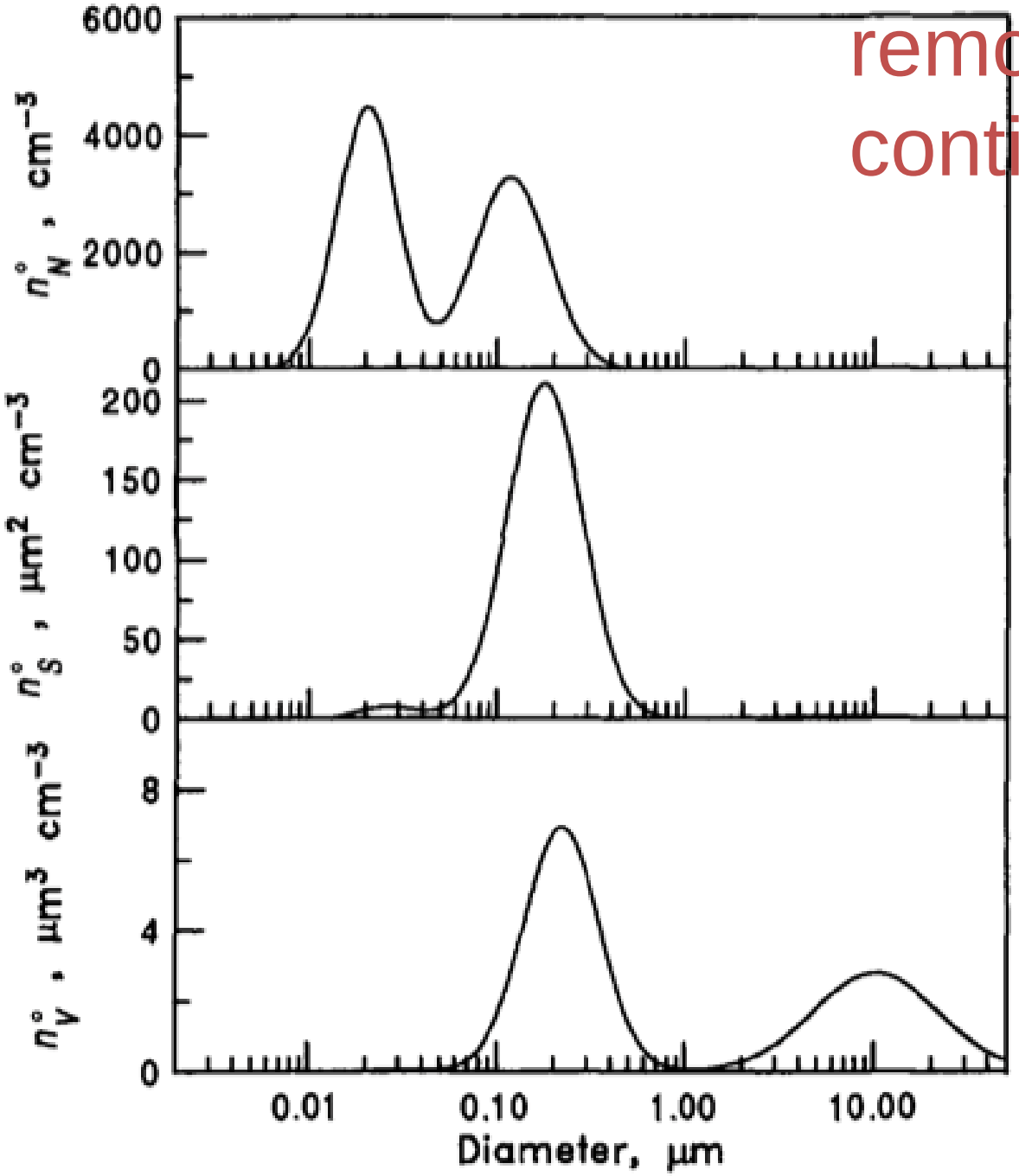

FIGURE 8.18 Typical remote continental aerosol number, surface, and volume distributions.

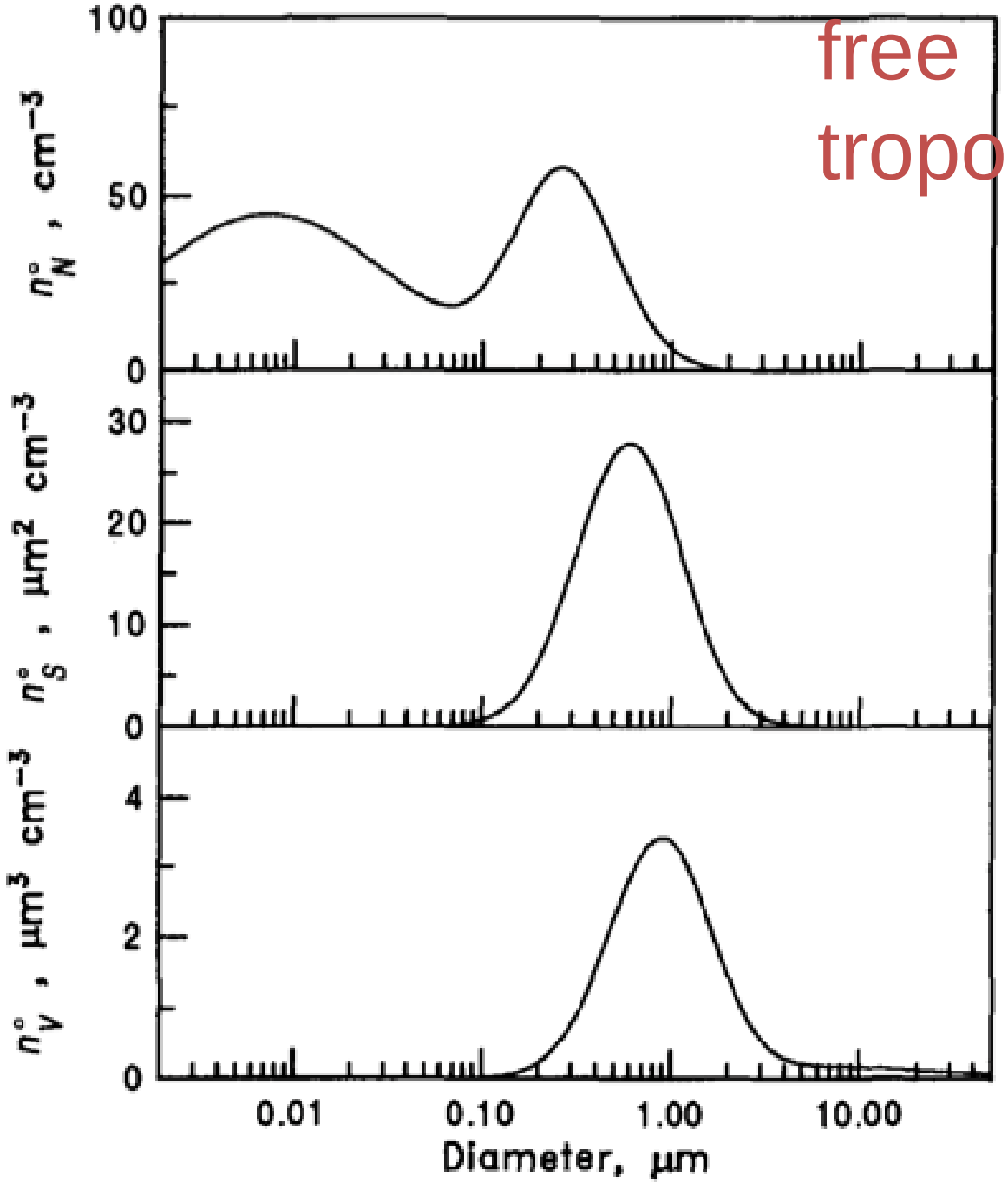

FIGURE 8.19 Typical free tropospheric aerosol number, surface, and volume distributions.

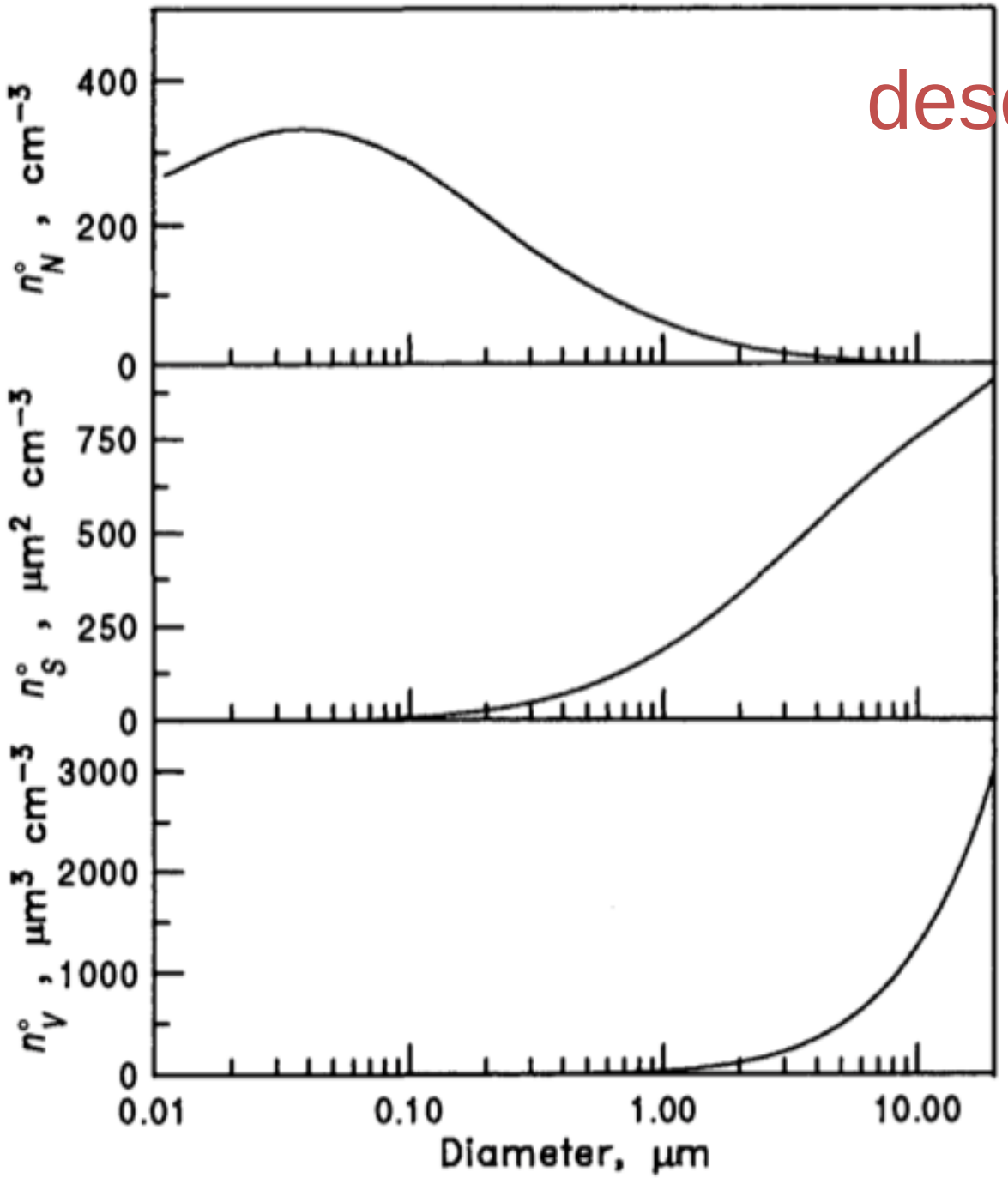

FIGURE 8.22 Typical desert aerosol number, surface, and volume distributions.

Filtration and gravimetry

Gravimetric mass analysis

- Sample collection on Teflon fiber or other type of filter ($PM_{2.5}$ or PM_{10} size cut)
- Filter is pre-weighed and post-weighed after conditioning at specific temperature and relative humidity
- Difference in filter weight indicates mass collected
- Standardized as the **Federal Reference Method (FRM)** in the United States, and is a standard method of measurement in other countries (though filter type and protocol varies)

https://metone.com/products/e-frm-dc-reference-method-particulate-sampler/
https://www.comde-derenda.com/en/products/mws-1/
https://asistec.ie/product/ultra-micro-micro-balances/

Inlet size selection

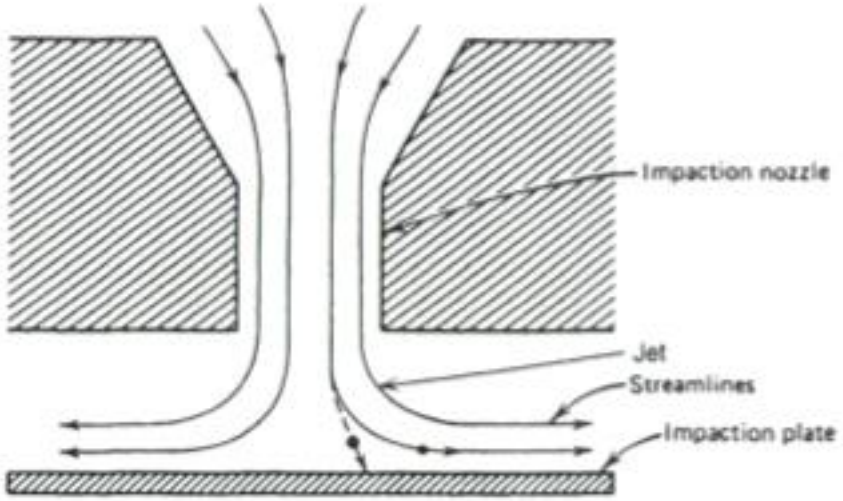

FIGURE 5.5 Cross-sectional view of an impactor.

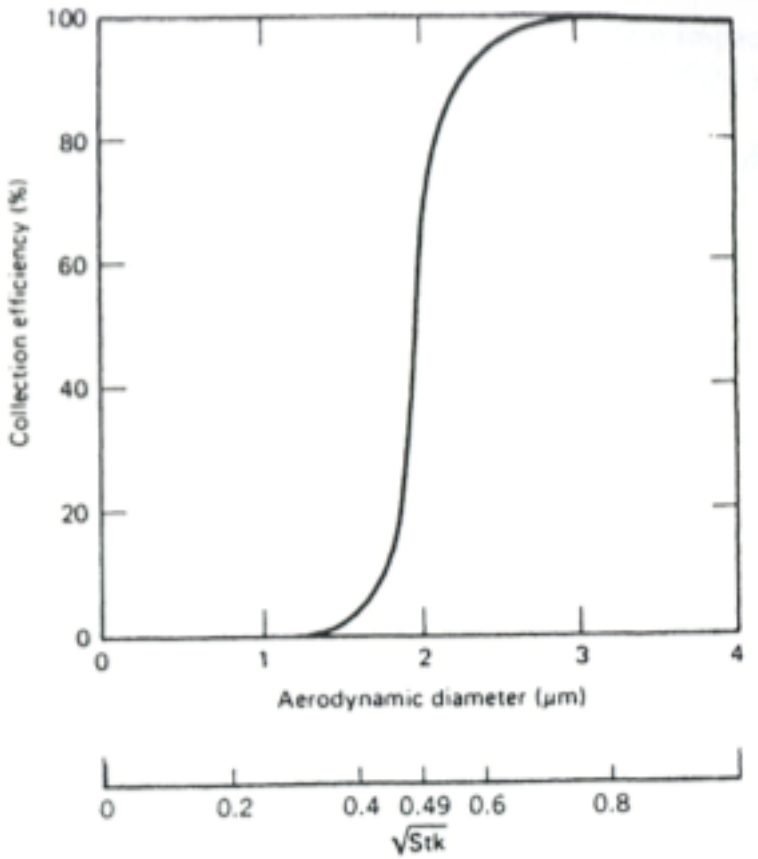

FIGURE 5.6 Typical impactor efficiency curve.

Hinds, *Aerosol science and Technology*, 1999

PM10 (particles < 10 µm)

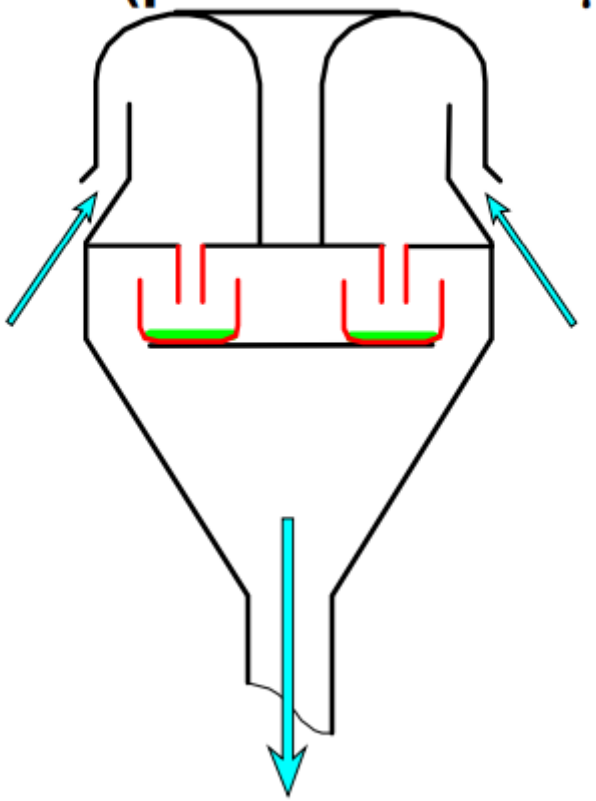

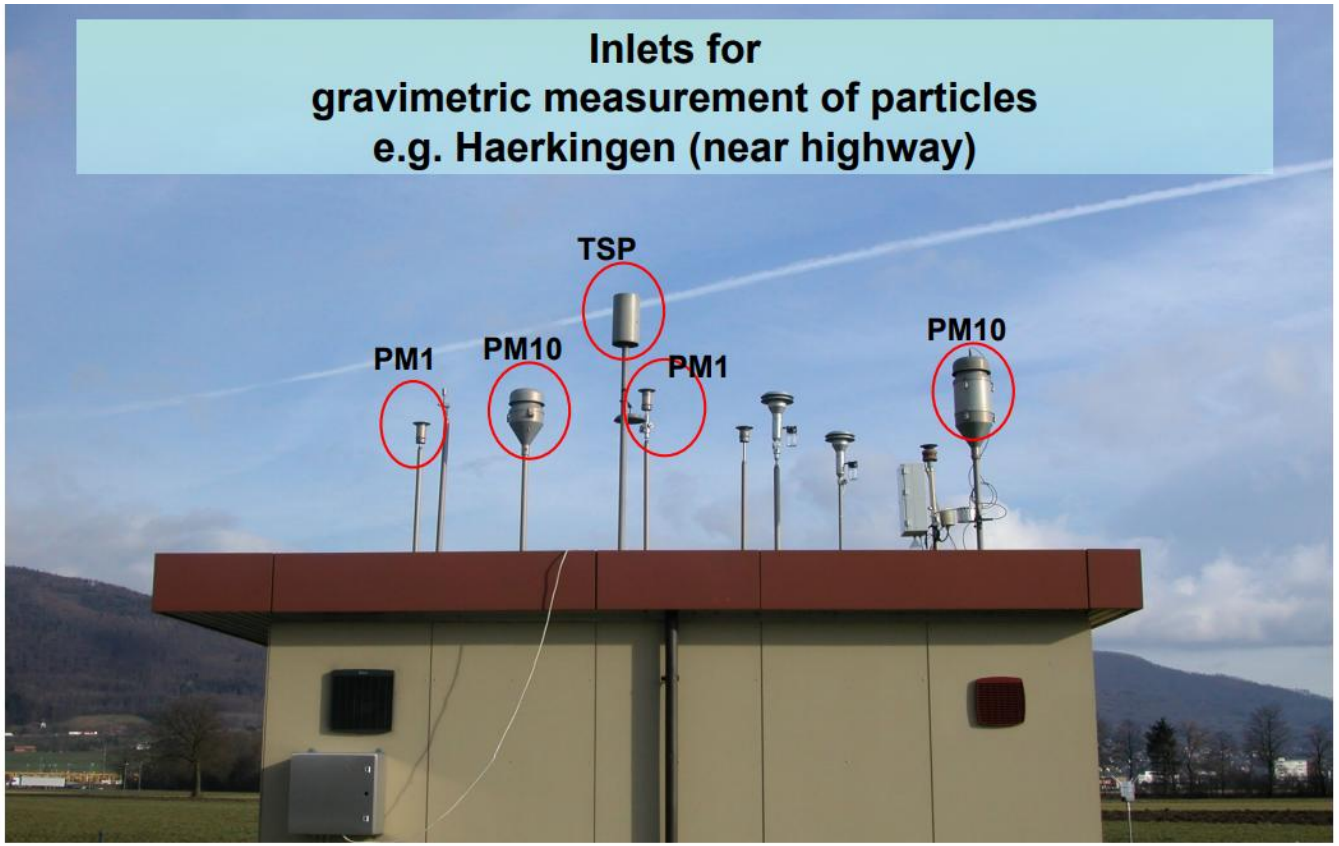

(from Stefan Reimann)

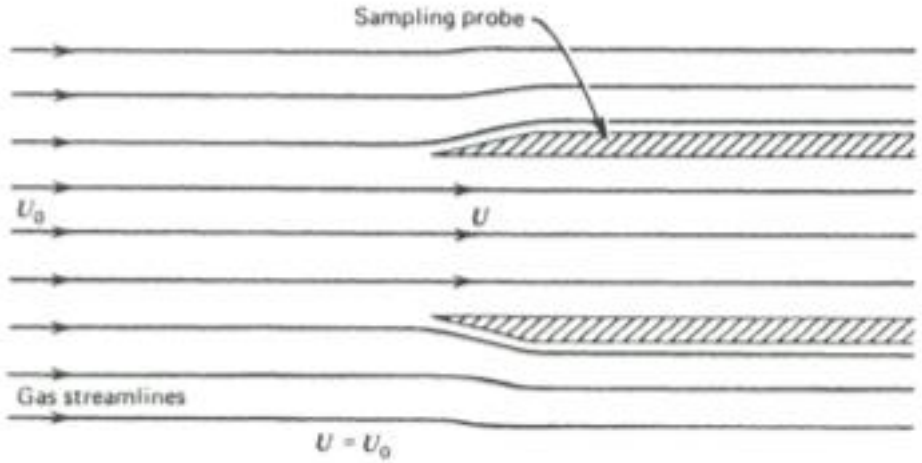

FIGURE 10.1 Isokinetic sampling.

Isokinetic inlets

When sampling aerosols:

- velocity of fluid in inlet has to match approaching fluid velocity
- → minimize particle losses/enrichment

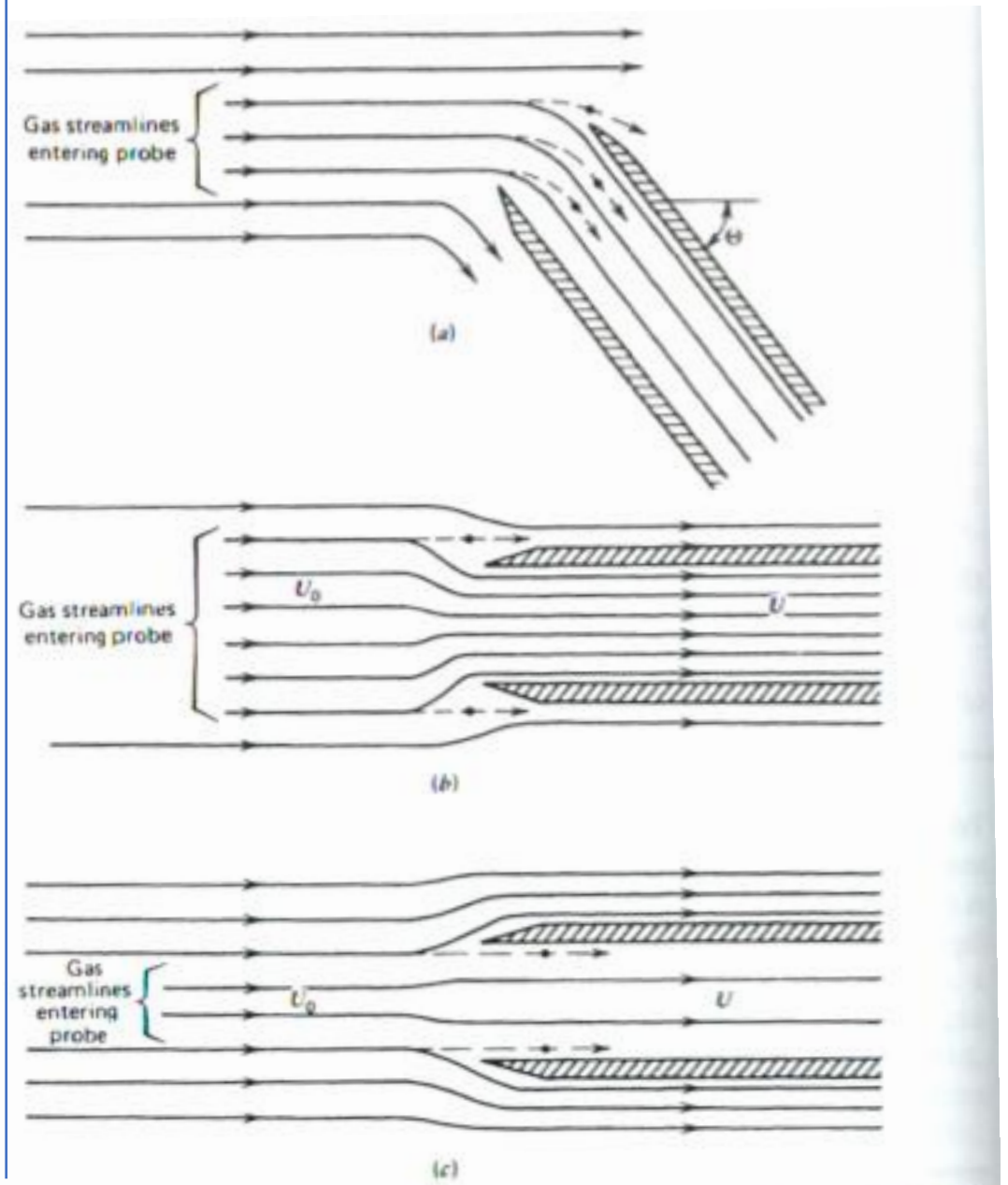

FIGURE 10.2 Anisokinetic sampling. (a) Misalignment, $\Theta \neq 0$. (b) Superisokinetic sampling, $U > U_0$. (c) Subisokinetic sampling, $U < U_0$.

Hinds, 1999

Consequences of non-isokinetic sampling

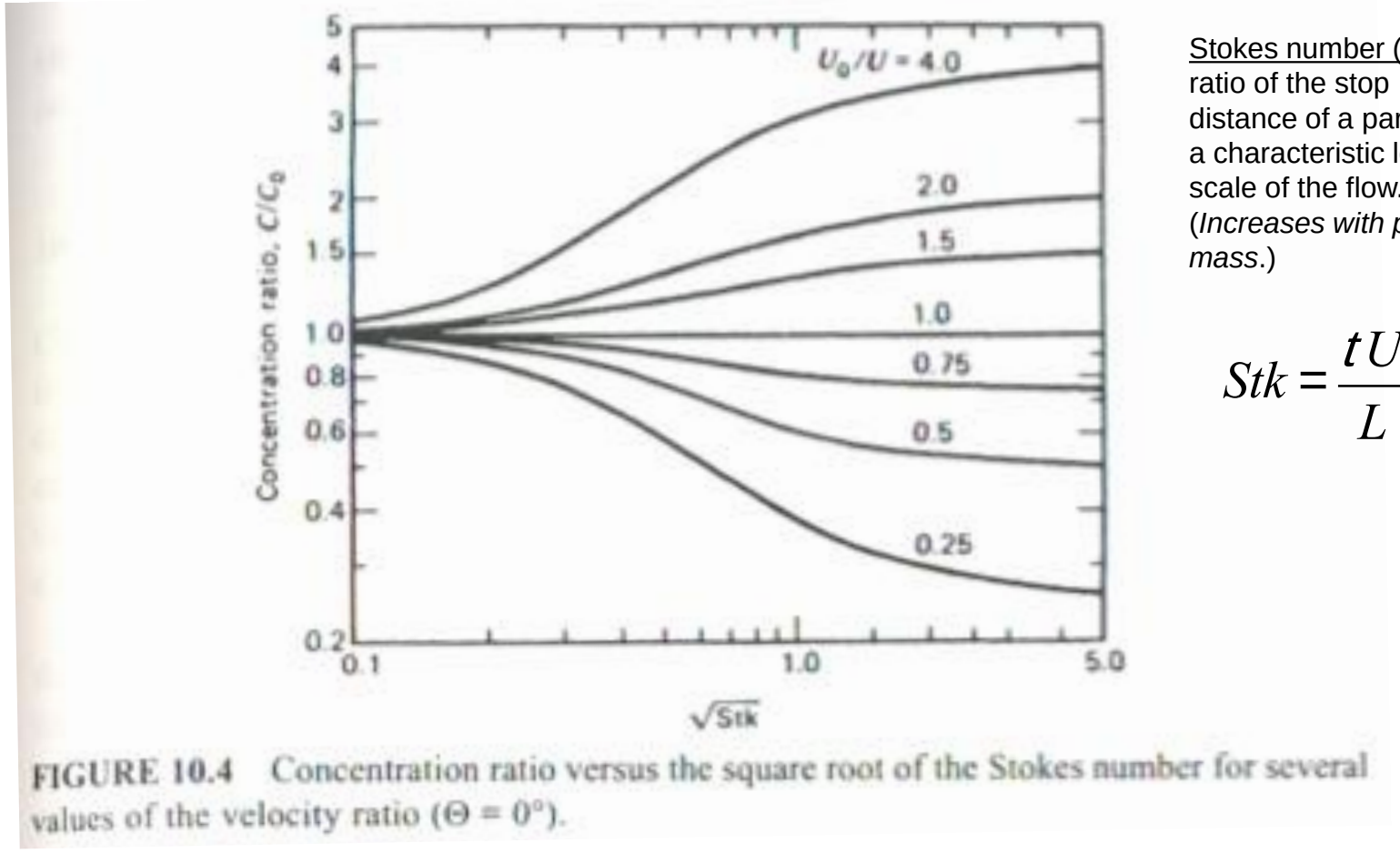

FIGURE 10.4 Concentration ratio versus the square root of the Stokes number for several values of the velocity ratio ($\Theta = 0°$).

Stokes number (Stk): ratio of the stop distance of a particle to a characteristic length scale of the flow. (*Increases with particle mass*.)

$$Stk = \frac{tU}{L}$$

Hinds, 1999

Especially important for aircraft sampling

http://eol.ucar.edu

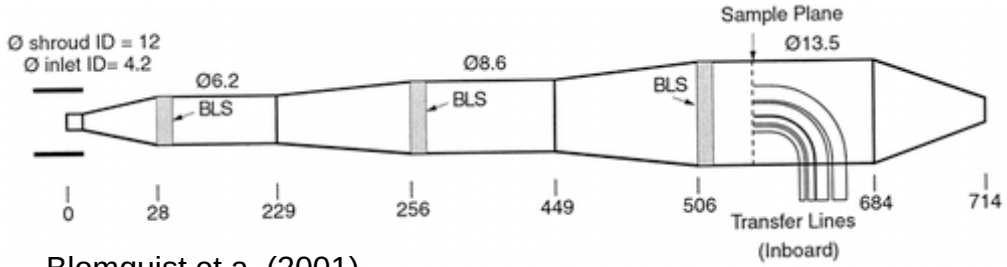

Blomquist et a. (2001)

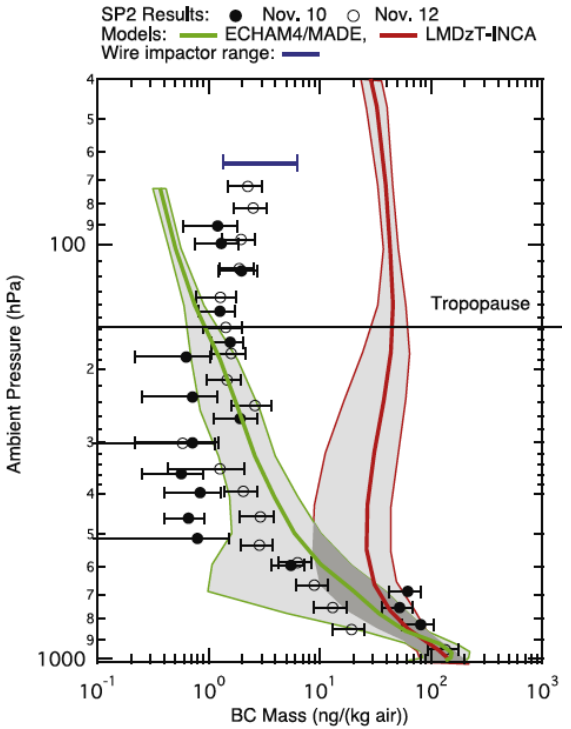

Aircraft measurements provide vertical concentration profiles (black carbon shown on right).

Schwarz et al., *Geophys. Res. Lett.*, 2006

Filter collection

Polyfluorotetraethylene or PTFE, Teflon® membrane filter

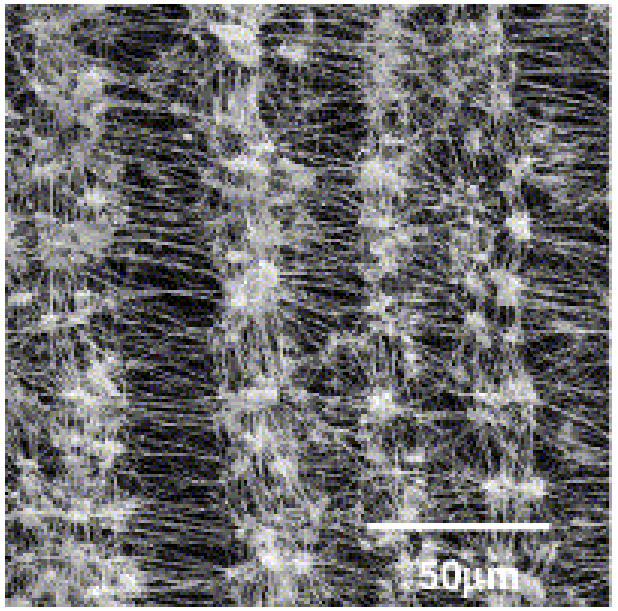

Casuccio et al., *Fuel Process Tech.*, 2004
https://scientificfilters.com/whatman/membranes-ptfe-membranes-7592-104

Filtration

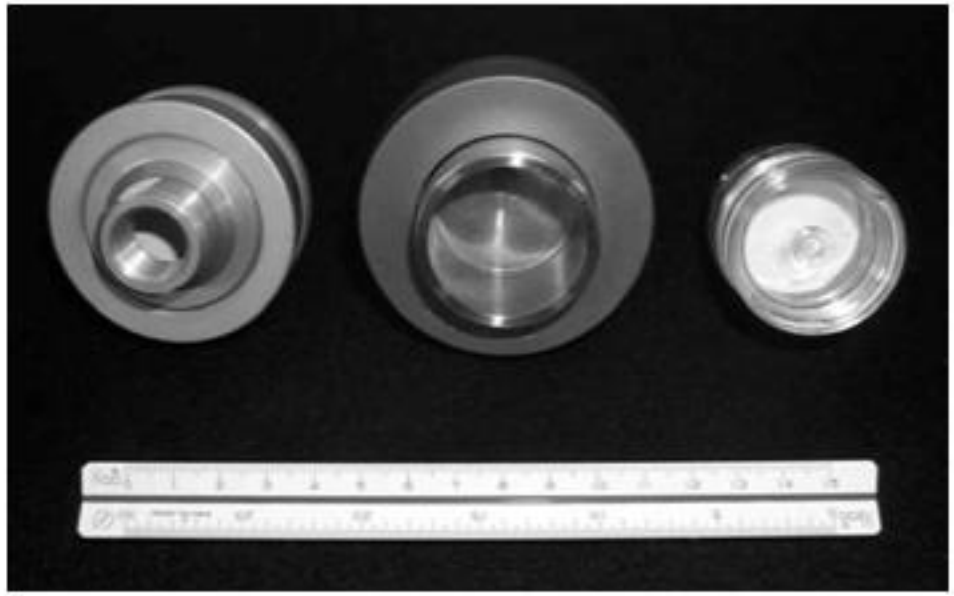

Figure 7-2 Examples of filter holders available commercially for aerosol collection (from left): in-line, ***GEL***, 47 mm; open-face, ***MIL***, 47 mm; and closed-face cassette, ***GEL***, 25 mm (can also be used open-faced). Photograph courtesy of H. T. Kim, Gwangju Institute of Science and Technology.

fibrous filter

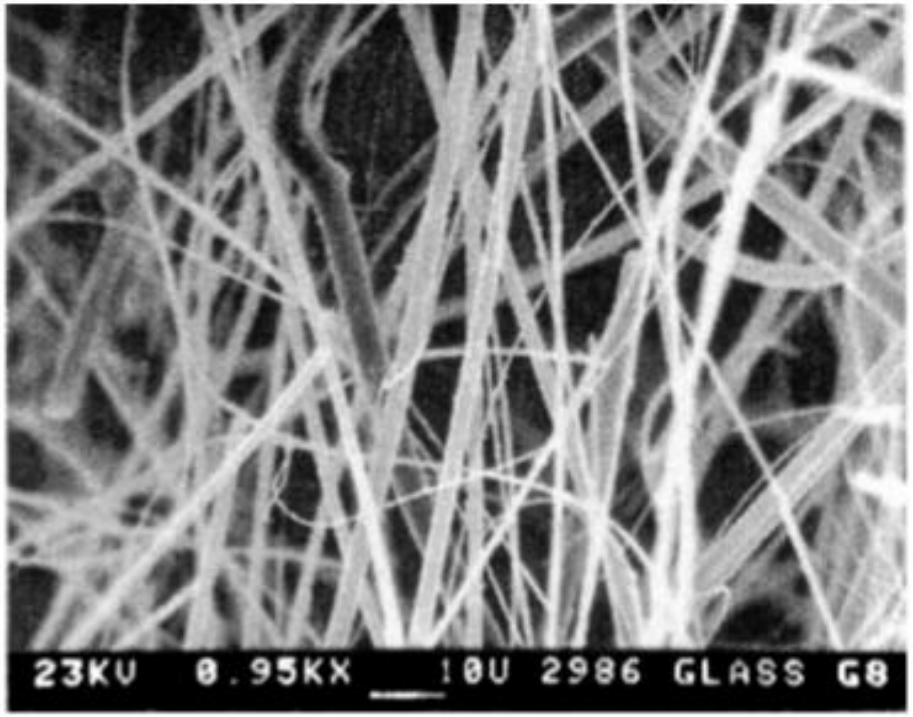

Figure 7-3 Electron micrograph showing the typical microstructure of a glass fiber filter (***GEL*** type A/E). Scale bar shown on the micrograph.

membrane filter

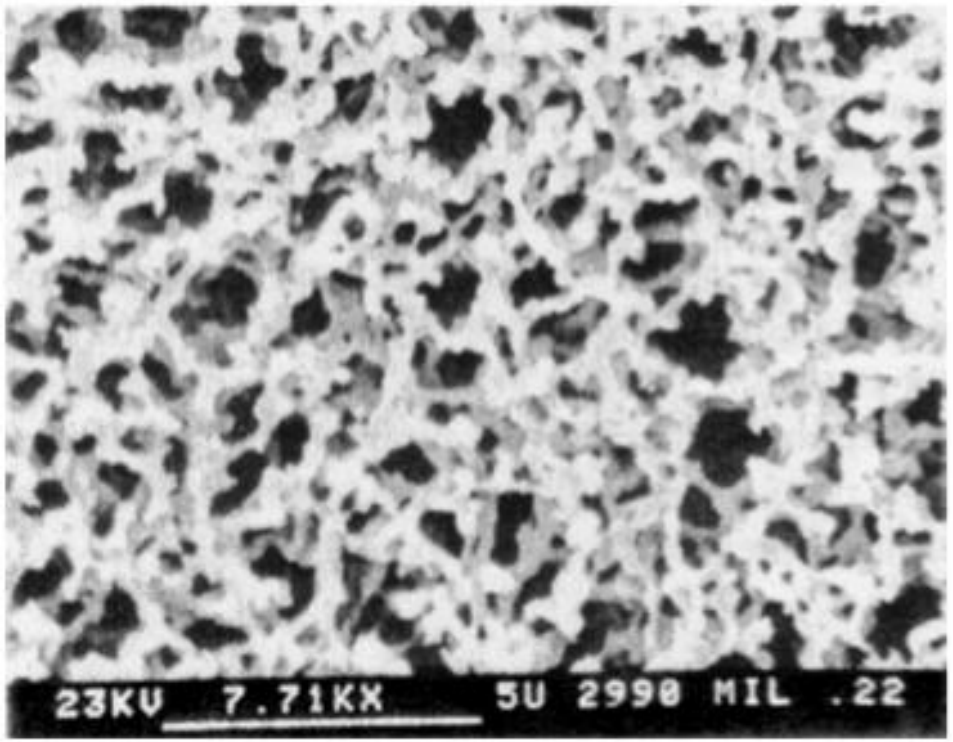

Figure 7-4 Electron micrograph of a membrane filter (*MIL*, 0.22-μm pore size) showing the tortuous flow path and structural elements in the filter. Scale bar shown on the micrograph.

pore filter

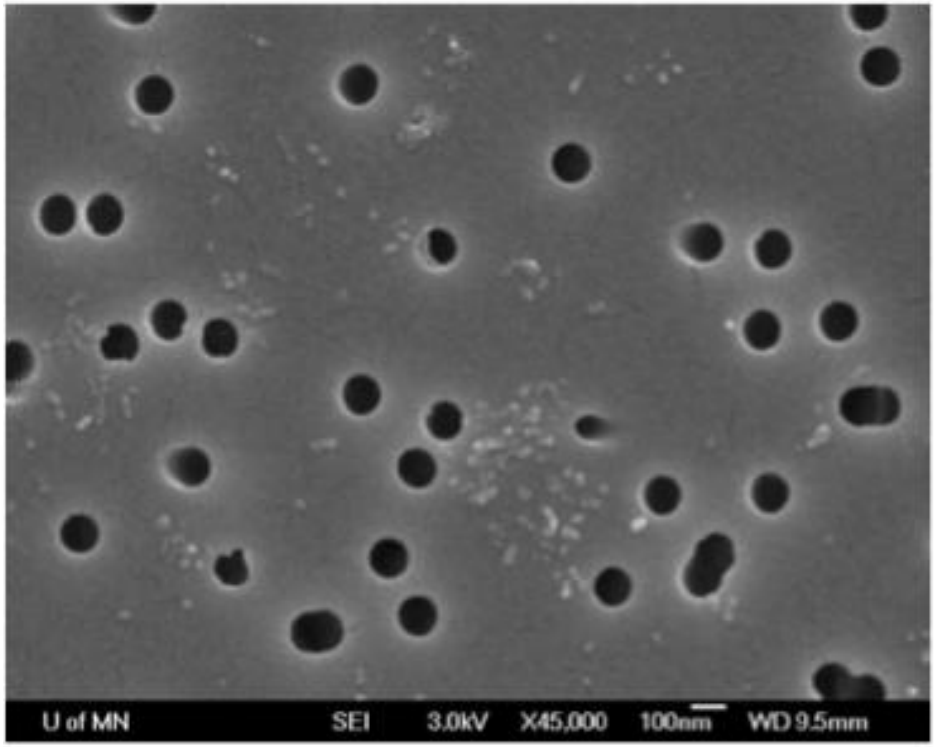

Figure 7-5 Electron micrograph of a capillary pore filter (*MIL* Isopore® polycarbonate, 0.1-μm pore size) showing the relatively smooth surface and uniform pores in the filter. Scale bar shown on micrograph.

Bag filter

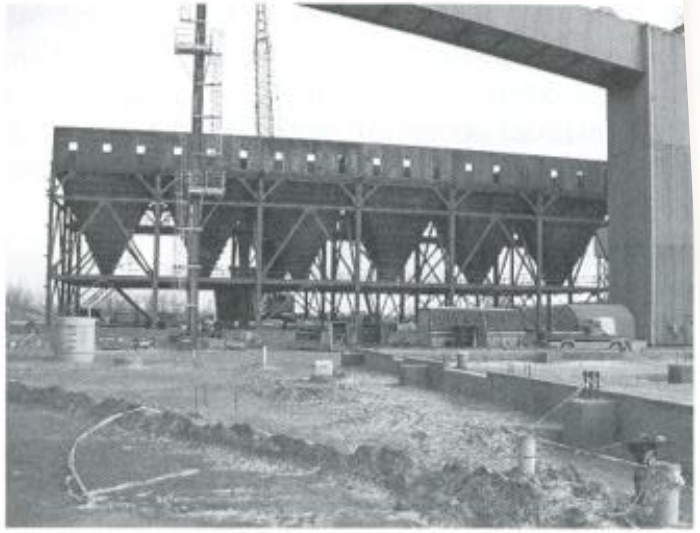

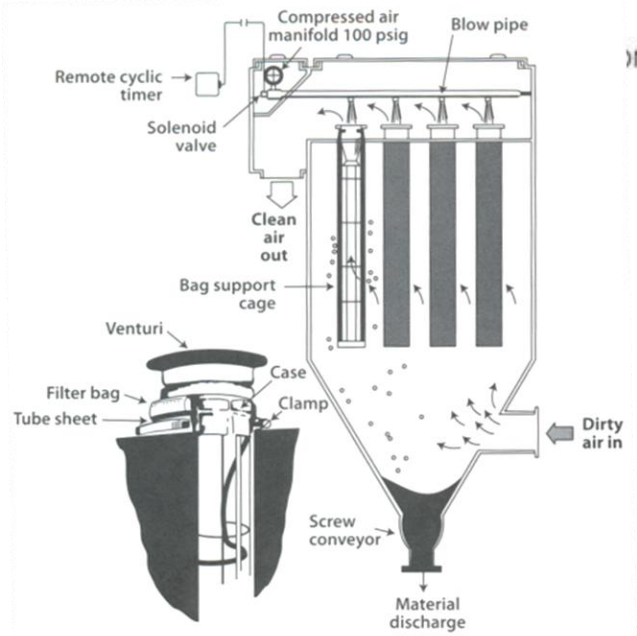

Figure 6.6
Schematic diagram of a pulse-jet baghouse.

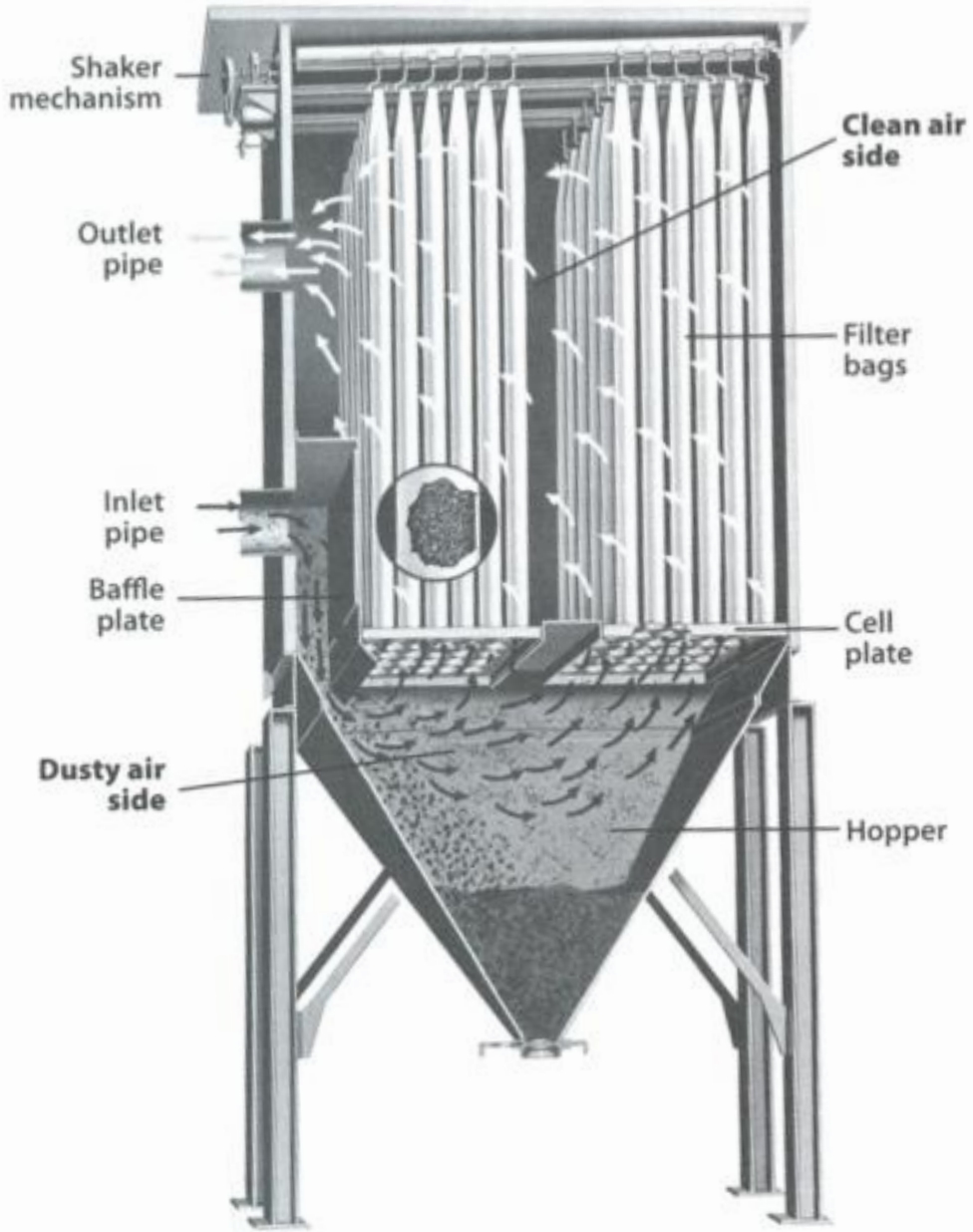

Figure 6.3
Cutaway view of a shaker baghouse.
(Courtesy of Siemens Energy, Inc., Orlando, FL.)

Cooper and Alley, 2006

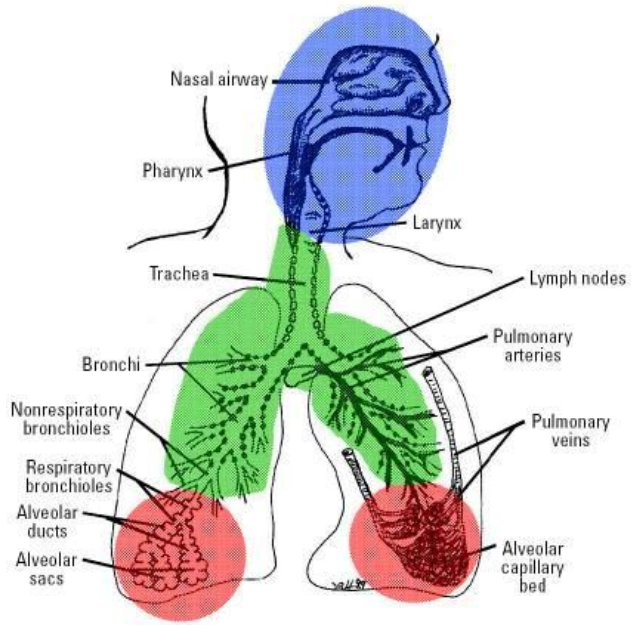

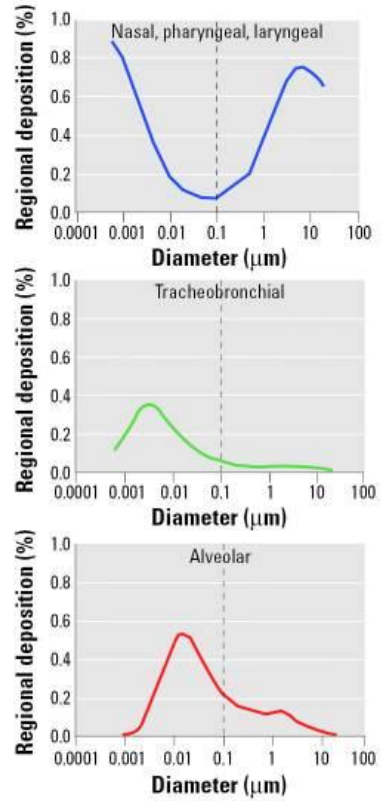

Nanotoxicology: An Emerging Discipline Evolving from Studies of Ultrafine Particles

Günter Oberdörster,[1] Eva Oberdörster,[2] and Jan Oberdörster[3]

[1]Department of Environmental Medicine, University of Rochester, Rochester, New York, USA; [2]Department of Biology, Southern Methodist University, Dallas, Texas, USA; [3]Toxicology Department, Bayer CropScience, Research Triangle Park, North Carolina, USA

Particle-fiber interactions

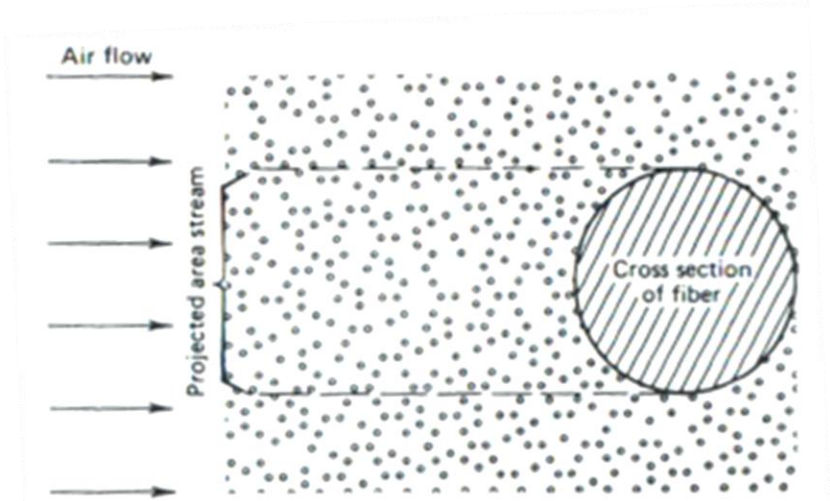

FIGURE 9.4 Single-fiber efficiency.

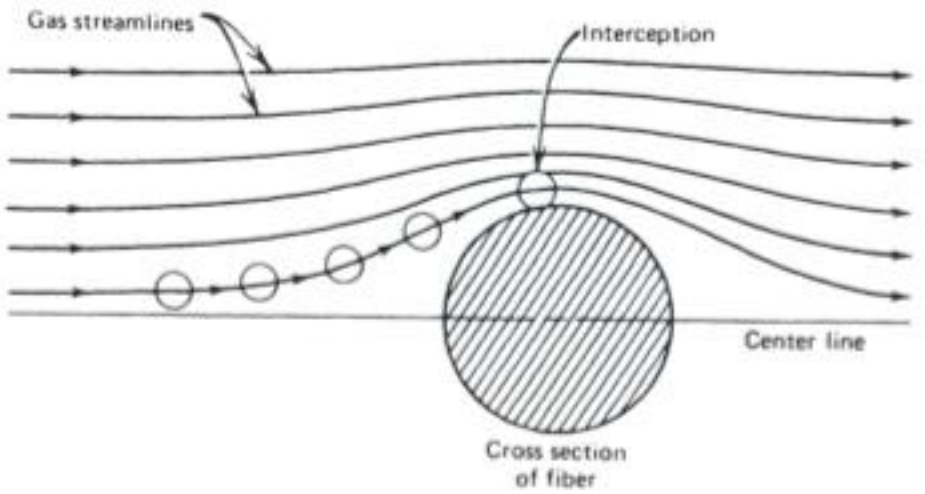

FIGURE 9.5 Single-fiber collection by interception.

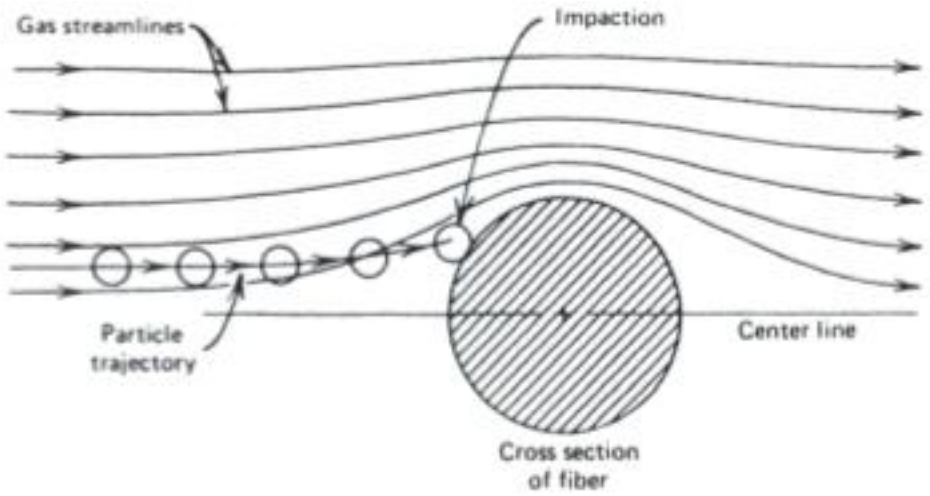

FIGURE 9.6 Single-fiber collection by impaction.

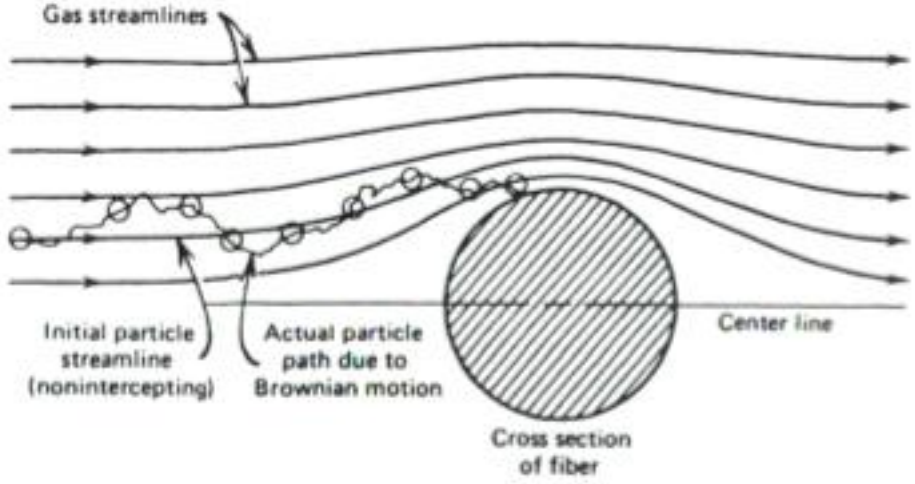

FIGURE 9.7 Single-fiber collection by diffusion.

Hinds, *Aerosol science and Technology*, 1999

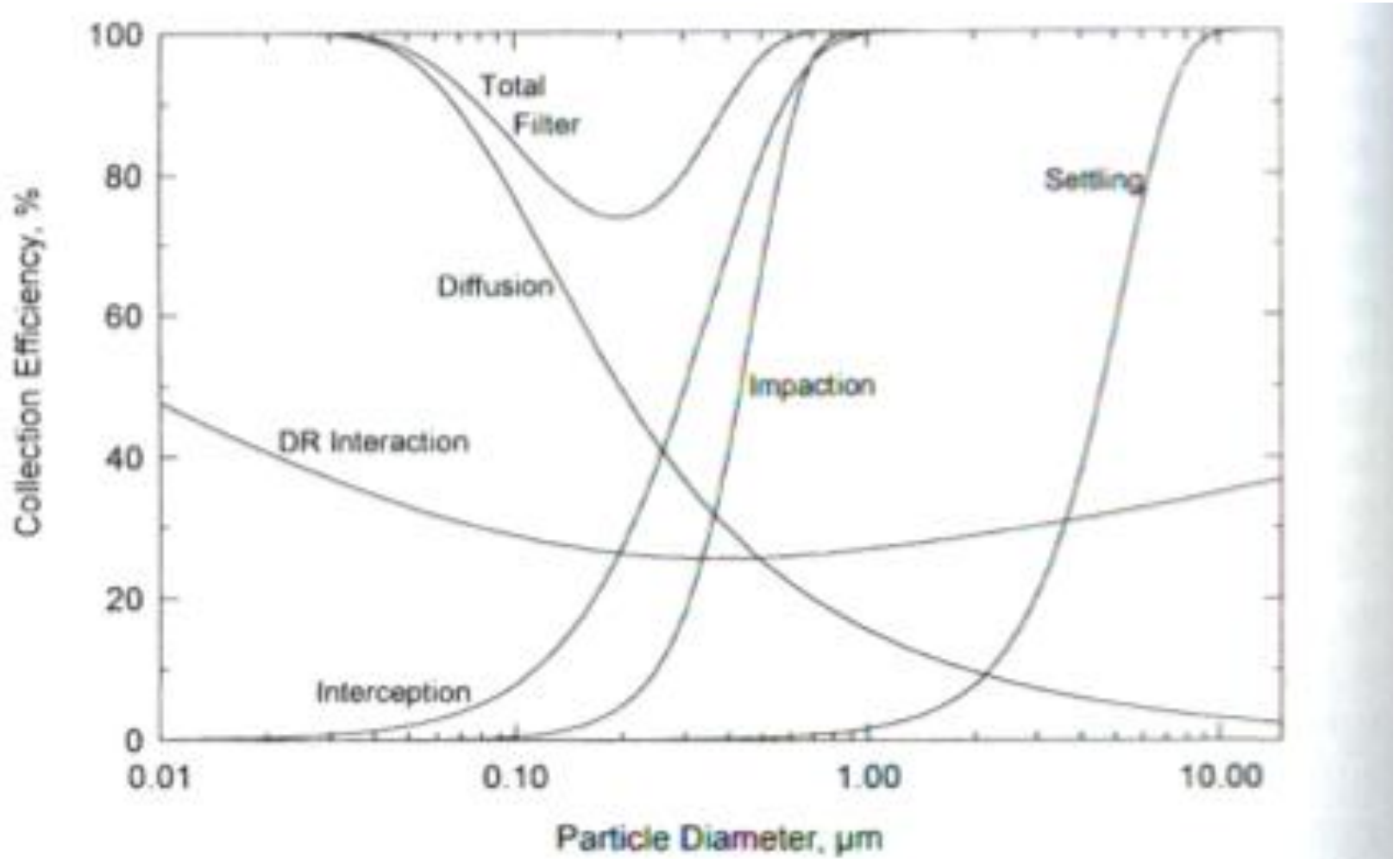

FIGURE 9.8 Filter efficiency for individual single-fiber mechanisms and total efficiency; $t = 1$ mm, $\alpha = 0.05$, $d_f = 2$ µm, and $U_0 = 0.10$ m/s. [10 cm/s].

Hinds, *Aerosol science and Technology*, 1999

Number vs volume size distribution

- Larger particles
  - far fewer in number
  - contribute much more toward mass concentrations
- Number weighted by diameter cubed (D_p^3)

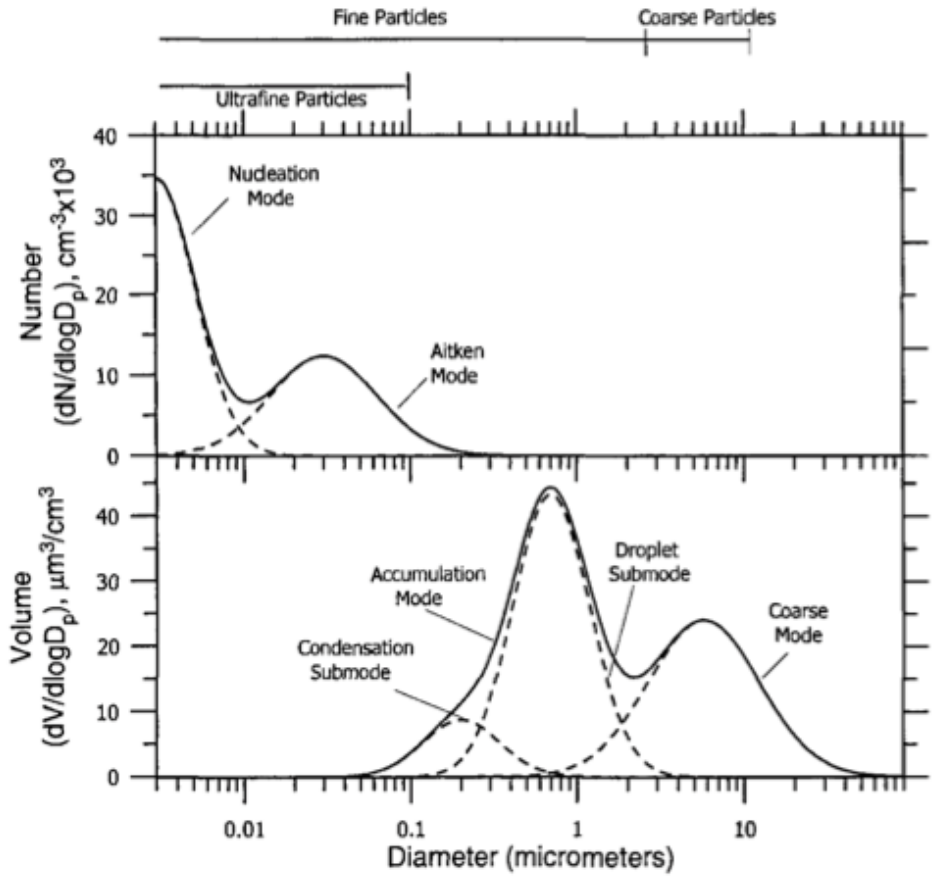

Seinfeld and Pandis, *Atmospheric Chemistry and Physics*, 2016

Chemical transformations on optical response and gravimetric measurements

Water uptake

- Relative humidity (RH) affects particle size and mass
- RH is sensitive to temperature – RH in Purple Air may not be same as ambient
- Gravimetric mass measurements are measured at a specified humidity (35-45% depending on protocol).

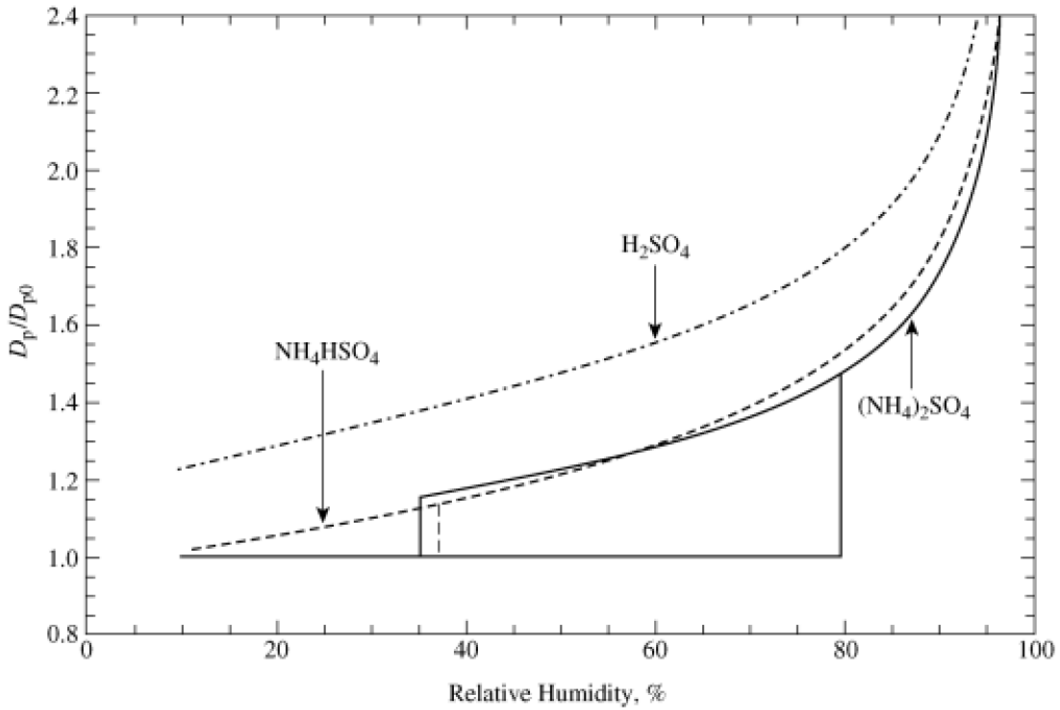

Seinfeld and Pandis, *Atmospheric Chemistry and Physics*, 2016

Evaporation and other artifacts

Sampling artifacts for gravimetric analysis assessed by comparing against sum of chemically speciated mass

- Retention of water
- Evaporative loss of semivolatile substances
- Adsorption of gases to filter media or collected particles

Chemical reactions (e.g., oxidation) can also affect the mechanisms above

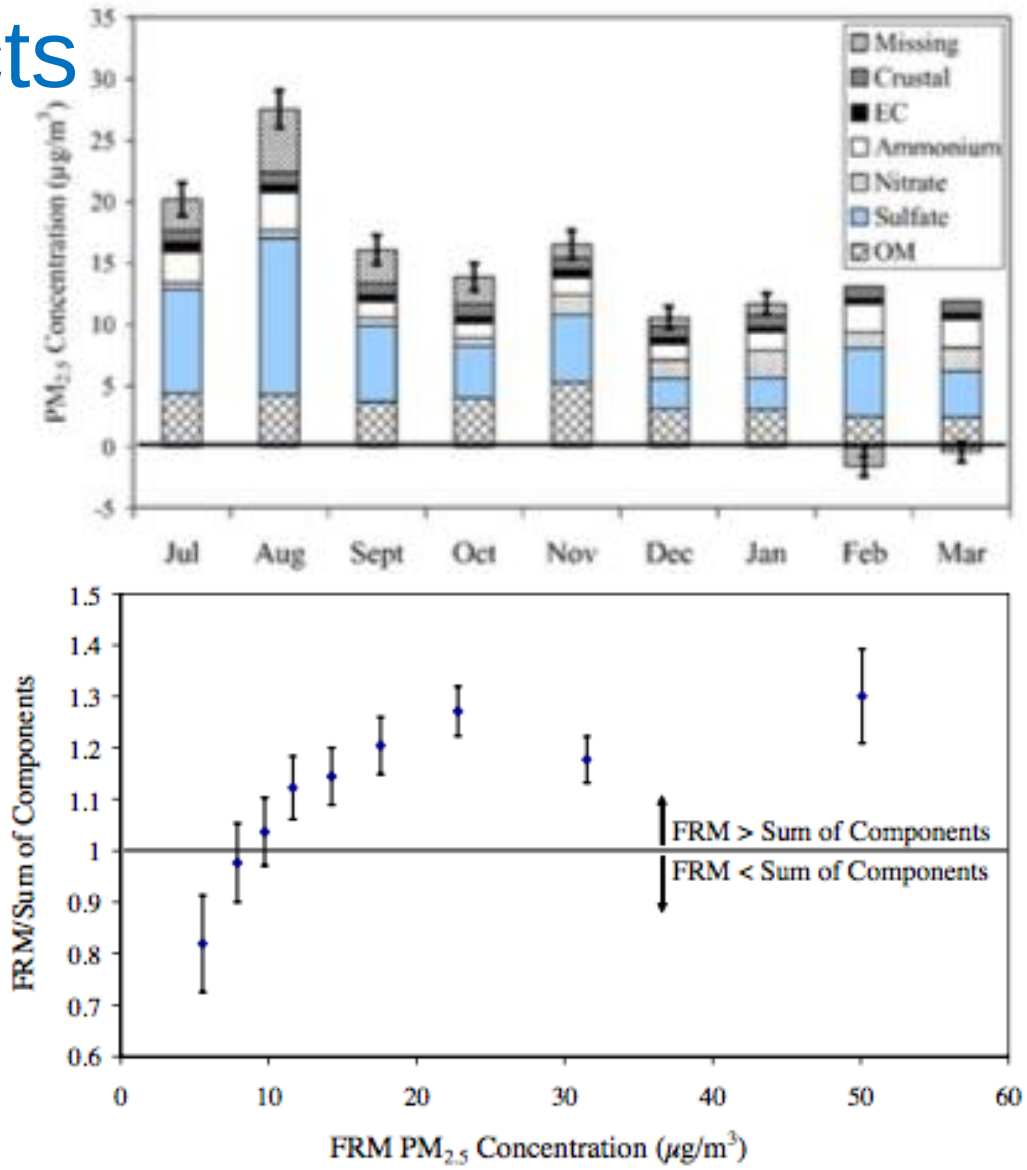

Rees et al., *Atmos. Environ.*, 2004

An automated gravimetric measurement

- Tapered Oscillating Element Microbalance
- Heated inlet to evaporate water
- Evaporates semivolatiles also

video link

Aerosol physics

Applications for sampling and particulate matter removal

- Impaction (size-selective inlets, sample collection, size classifiers)
  - inertial impaction (particle trajectory deviates from fluid streamline due to particle inertia)
  - an example from Seinfeld and Pandis (2006) is presented later
- Filtration (sample collection filters, bag houses)
  - inertial impaction (particle trajectory deviates from fluid streamline due to particle inertia)
  - interception (particle trajectory follows streamline but still collides with object because of particle size)
  - diffusion from Brownian motion
- Electrostatic selection (measurement/particle removal devices)
  - Electrostatic size classifiers
  - Electrostatic precipitators

Principles of aerosol measurement and emission control

Mechanical/physical

- filtration
- gravimetric analysis
- thermal separation
- absorption/adsorption
- charge separation

Chemical

- dissolution
- extraction
- reaction

Continuum description of flow

Kulkarni et al., 2011

Continuity $\nabla \cdot \mathbf{u} = 0$

Navier Stokes (conservation of momentum)

$$\rho_g \frac{D\mathbf{u}}{Dt} = \underbrace{\rho_g \left(\frac{\partial \mathbf{u}}{\partial t} + \mathbf{u} \cdot \nabla \mathbf{u} \right)}_{\text{inertial forces}} = \underbrace{-\nabla p}_{\text{Forces from pressure gradient}} + \underbrace{\mu \nabla^2 \mathbf{u}}_{\text{Viscous shear forces}}$$

Incompressible flow $Ma = \frac{U}{U_{\text{sonic}}} \ll 1$

Equation of state (ideal gas law) $p = \frac{\rho_g RT}{M}$

Gas Viscosity μ

At standard conditions (293K, 101 kPa):
$\mu = 1.81 \times 10^{-5}$ Pascale-second

Reynolds number $Re = \frac{\rho UL}{\mu} = \frac{UL}{\nu}$

Note L can be different according to application:

- Flow in tube, $L = D$; flow Reynold's number Re_f
- Flow around particle, $L = D_p$; particle Reynold's number Re_p

Momentum conservation on a single particle

$$m_p \frac{d\mathbf{v}}{dt} = \sum_i \mathbf{F}_i$$

v is the particle velocity vector
u is the fluid velocity vector
m_p is the particle mass
F is the force vector

$$\mathbf{F}_{\text{drag}} = \frac{3\pi\mu D_p}{C_c}(\mathbf{u} - \mathbf{v})$$

$$\mathbf{F}_{\text{gravitational}} = m_p\mathbf{g}$$

$$\mathbf{F}_{\text{Brownian}} = m_p\mathbf{a}$$

$$\mathbf{F}_{\text{electrostatic}} = q\mathbf{E}$$

...

…Additional mechanisms:

- *thermophoresis*
  (motion of molecules caused by heat gradient)
- *photophoresis*
  (motion of molecules caused by heat gradient)
- *electromagnetic radiation pressure*
  (momentum transfer from EMR)
- *acoustic pressure*
- *diffusiophoresis*

Drag force

- The expression for drag force on a single particle is derived from Stokes' law for low flow conditions (viscous forces dominate; neglect inertial forces).
- The *Cunningham slip-correction factor* is introduced to account for the fact that when the particle size approaches the mean free path of the gas, no-slip boundary condition for which the equations of flow were derived (by Stokes' law) do not necessarily apply.

Derivation of **drag force** from Stokes' law (continuum regime, low flow)

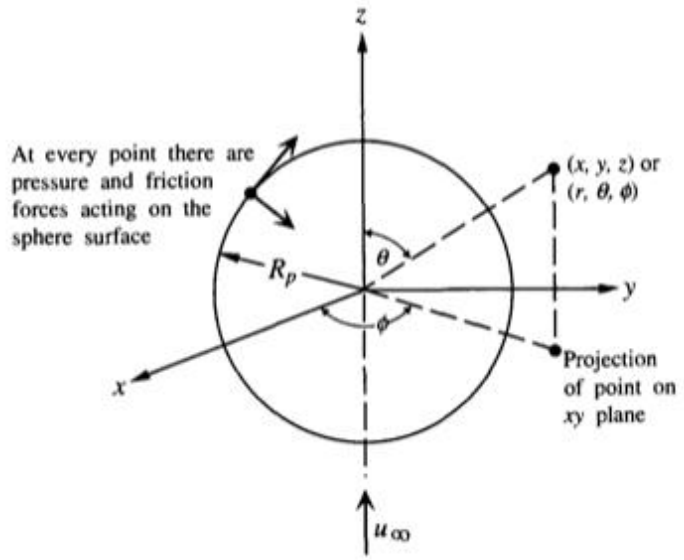

Seinfeld and Pandis (2006)

For steady, incompressible flow with negligible inertial forces, the continuity and Navier-Stokes equations are as follows:

$$\nabla \cdot \mathbf{u} = 0$$

$$\nabla p = \mu \nabla^2(\mathbf{u})$$

We get p from solution of the equations above (with boundary conditions $u|_{r=R_p} = 0$ and $u|_{r\to\infty} = u_\infty$; neglecting gravity); τ from Newton's Law of viscosity:

$$p = p_0 - \frac{3}{2}\frac{\mu u_\infty}{R_p}\left(\frac{R_p}{r}\right)^2 \cos\theta$$

$$\tau = \frac{3}{2}\frac{\mu u_\infty}{R_p}\left(\frac{R_p}{r}\right)^4 \sin\theta$$

Expressions for forces arising from pressure acting perpendicularly and shear stress acting tangentially to the surface of a sphere:

$$F_n = \int\int_S \left(-p|_{r=R_p} \cos\theta\right) dS$$

$$F_t = \int\int_S \left(\tau|_{r=R_p} \sin\theta\right) dS$$

where $dS = R_p^2 \sin\theta d\theta d\phi$.

The net (overall drag) force is the sum of the normal and tangential forces ("form" and "friction" drag, respectively):

$$F_D = F_n + F_t = 6\pi\mu u_\infty R_p = 3\pi\mu u_\infty D_p$$ Bird et al. (1960)

See also Bird, Stewart, and Lightfoot *Transport Phenomena*, 2007

Regimes of fluid-particle interactions

When the particle radius approaches the mean free path of the surrounding fluid (gas), the description of the interacting fluid as a continuum as to be revisited.

Knudsen number $$Kn = \frac{\lambda}{R_p} = \frac{2\lambda}{D_p}$$

Mean free path of air at standard conditions (293K, 101 kPa): λ = 0.066 μm

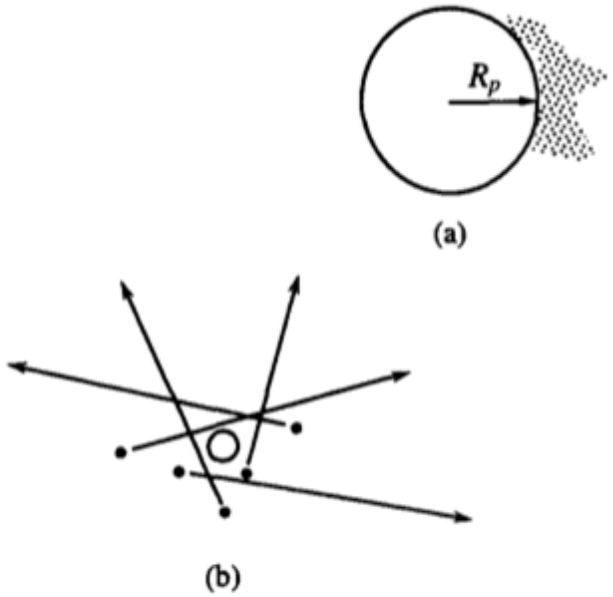

FIGURE 9.1 Schematic of the three regimes of suspending fluid–particle interactions: (a) continuum regime (Kn → 0), (b) free molecule (kinetic) regime (Kn → ∞), and (c) transition regime (Kn ~ 1).

Seinfeld and Pandis (2006)

Drag force with slip correction

Stokes' law was used to derive the expression for creeping flow around a stationary sphere (low $Re \leq 1$; $Kn \gg 1$; fluid velocity u_∞). Under conditions for which Knapproaches 1 or less, we introduce the Cunningham slip correction factor, C_c:

$$F_{\text{drag}} = \frac{3\pi\mu u_\infty D_p}{C_c}$$

The Cunningham slip correction factor is written as

$$C_c = 1 + Kn\,[1.257 + 0.4\exp(-1.1/Kn)]$$

Regime	Slip correction approximation
$Kn \gg 1$	$C_c \approx 2.154Kn/2$
$Kn > 10$	$C_c \approx 1.700Kn$

When the particle is in motion with velocity **v** within the fluid of velocity **u**, we can write the net drag force vector as

$$\mathbf{F}_{\text{drag}} = \frac{3\pi\mu D_p}{C_c}(\mathbf{u} - \mathbf{v})$$

Kulkarni et al., 2011

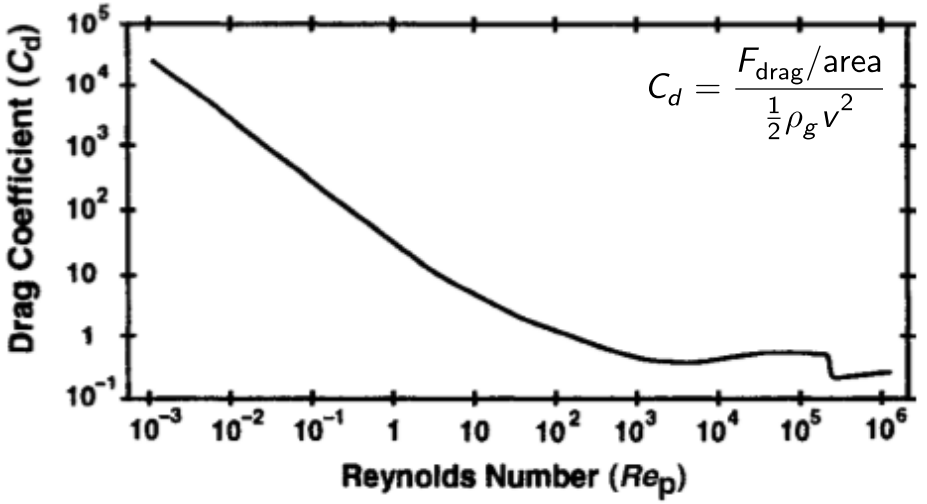

Figure 2-2 Drag coefficient as a function of particle Reynolds number for spherical particles.

Gravitational settling

- In the absence of other forces, the motion of a particle subjected to a gravity field can be described by the balance of drag and gravitational force.
- Settling velocities (rate of deposition due to gravitational force) can be calculated from this equation of motion, and it is shown that larger particles have a settling velocity orders of magnitude greater than smaller particles (both “small” and “large” referring to extremes in size of particles found in the atmosphere).

Gravitational settling example

Gravitational force:

$$\mathbf{F}_{\text{gravity}} = m_p \mathbf{g}$$

Momentum balance

$$m_p \frac{d\mathbf{v}}{dt} = \mathbf{F}_{\text{drag}} + \mathbf{F}_{\text{gravity}}$$
$$= \frac{3\pi\mu D_p}{C_c}(\mathbf{u} - \mathbf{v}) + m_p \mathbf{g}$$

Terminal velocity:

- Consider velocities only in z-direction
- $d\mathbf{v}/dt = 0$
- $\mathbf{u} = 0$ (or $\mathbf{u} \ll \mathbf{v}$)

Final expression:

$$v_{\text{terminal}} = \frac{m_p g C_c}{3\pi\mu D_p} \cdot \frac{D_p^2/4}{D_p^2/4} = \frac{1}{18}\frac{D_p^2 \rho_p g C_c}{\mu}$$

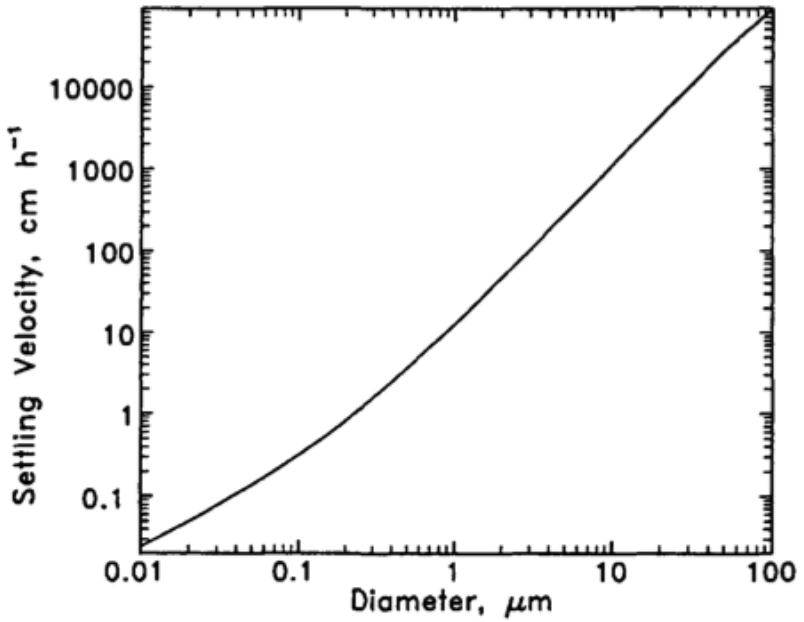

FIGURE 9.6 Settling velocity of particles in air at 298 K as a function of their diameter.

Seinfeld and Pandis (2006)

Brownian motion

- Originates from random collision of molecules in motion.
- The diffusion coefficient for particles can be derived from Fick's second law and equations of motion for a single particle (see Seinfeld and Pandis, 2006, Friedlander, 2000).

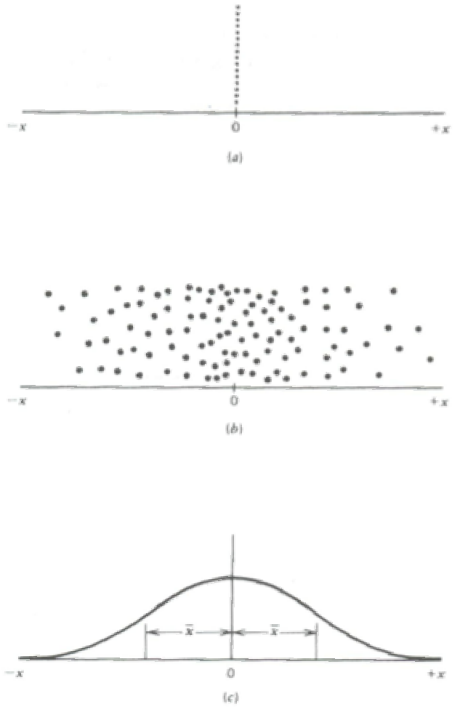

$$\frac{\partial n}{\partial t} = D\frac{\partial^2 n}{\partial x^2}$$

Hinds, *Aerosol Science and Technology*, 1999

Brownian diffusion

Seinfeld and Pandis (2006)

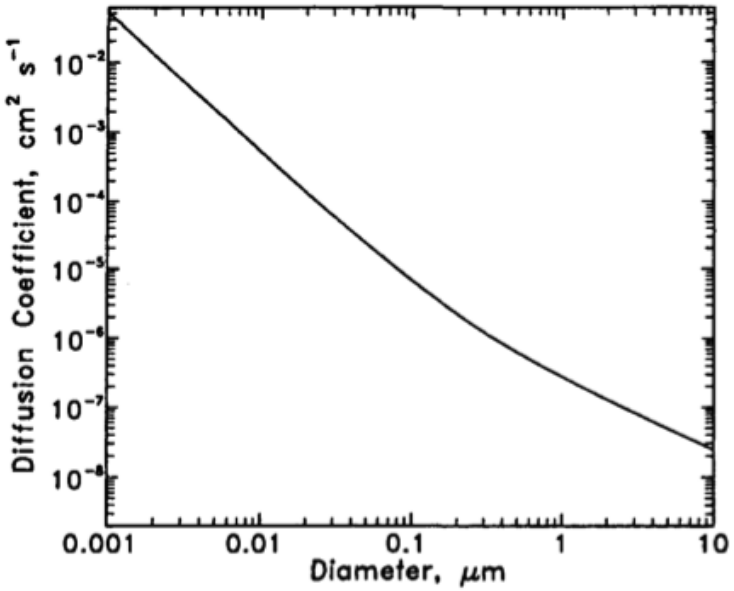

FIGURE 9.8 Aerosol diffusion coefficients in air at 20°C as a function of diameter.

Brownian or diffusion force is that exerted by randomly colliding molecules. The concentration gradient results in a net pressure translated into force:

$$\mathbf{F}_{\text{Brownian}} = -\frac{kT}{n}\nabla n$$

n is the number concentration of particles, k is the Boltzmann's constant, and T is the temperature.

The diffusion force results in a net particle motion resisted by Stokes drag:

$$m_p \frac{d\mathbf{v}}{dt} = \mathbf{F}_{\text{drag}} + \mathbf{F}_{\text{Brownian}}$$

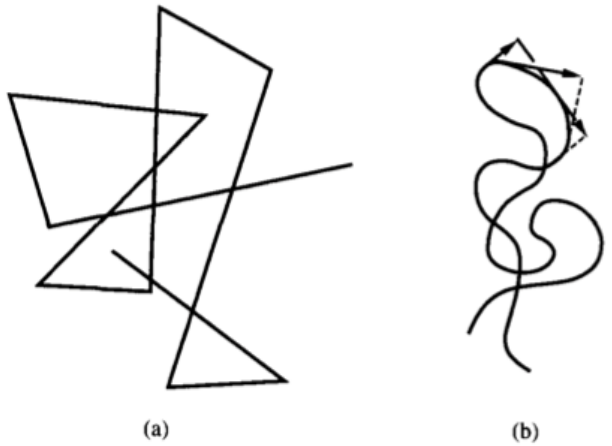

FIGURE 9.11 A two-dimensional projection of the path of (a) an air molecule and (b) the center of a 1-μm particle. Also shown is the apparent mean free path of the particle.

Note the dependence of the diffusion coefficient on particle size, D_p. *A 0.01 μm particle will be transported by diffusion 20,000 times faster than a 10 μm particle.*

Electrostatic force

The electrostatic force arises from

- a voltage gradient (which gives rise to an electrostatic field)
- charge on a particle

$$\mathbf{F}_{\text{electrostatic}} = q\mathbf{E}$$

$$\mathbf{E} = -\nabla V$$

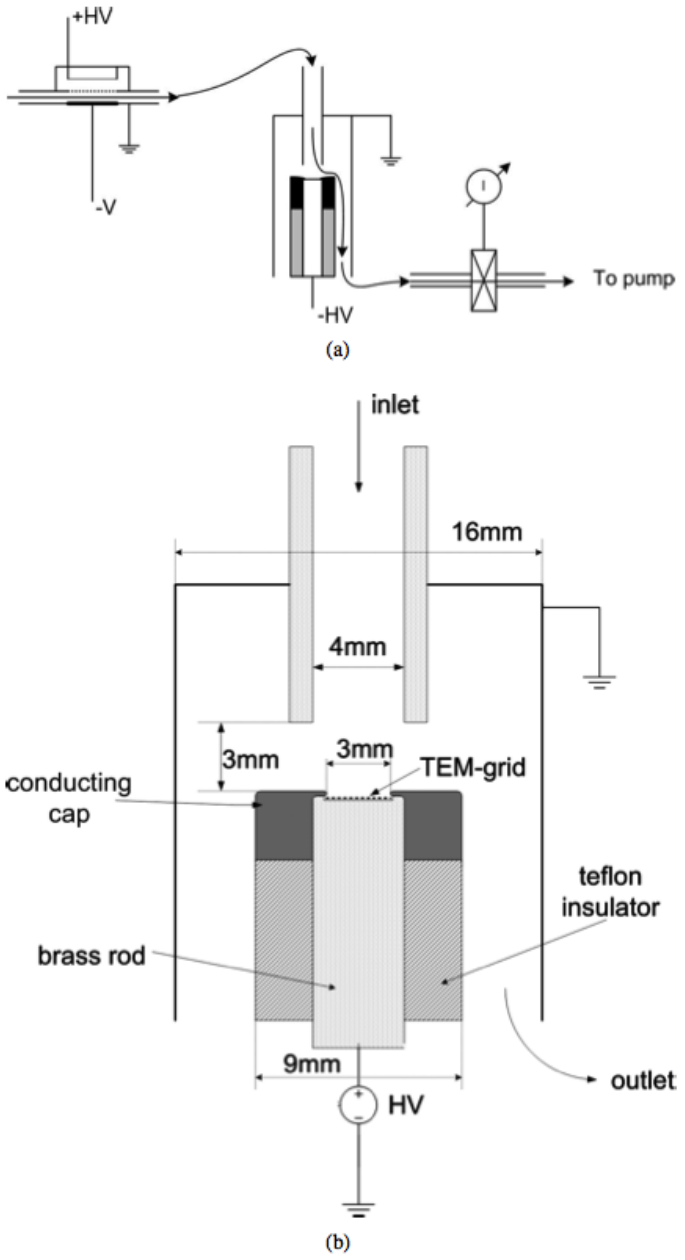

FIG. 1. (a) Principle of the TEM-sampler: Aerosol is charged in a Hewitt-type unipolar diffusion charger. The TEM grid is placed on a grid holder to which a negative high voltage is applied. The grid is held in place with a cap (shown in black). Charged particles are deposited on the TEM grid by electrostatic force, and remaining particles are measured in an aerosol electrometer. (b) Detail view of the sampling zone.

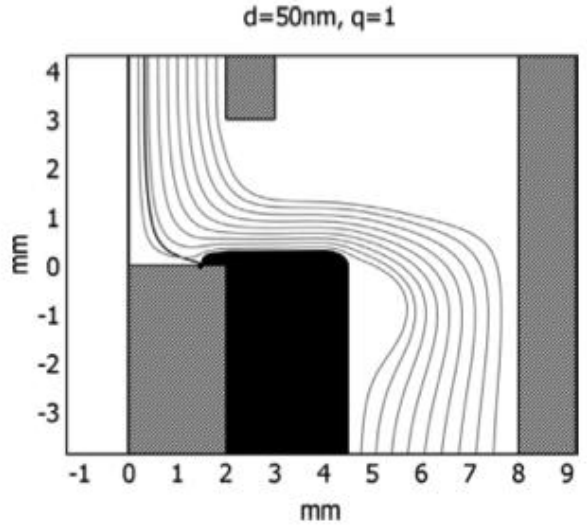

FIG. 2. Geometry of the Sampler and flow streamlines. The geometry has a rotational symmetry around the axis x = 0 mm. The TEM grid is placed on the grid holder in the y = 0 mm plane, and held in place by the cap (shown in black). The thick line is the trajectory of a particle of 50 nm diameter with one elementary charge released at r = R_c.

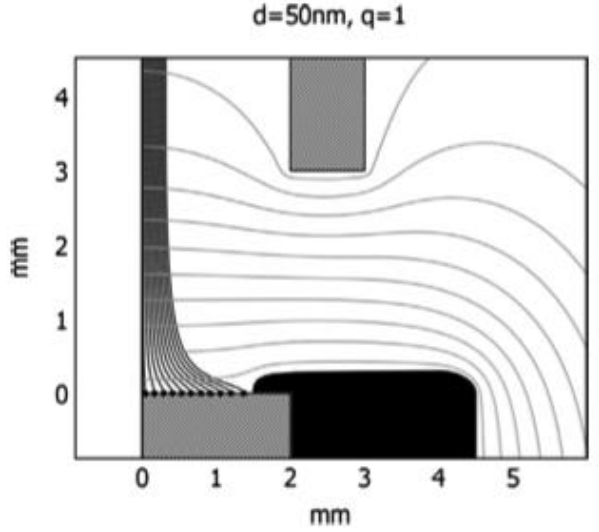

FIG. 3. Particle trajectories and equipotential lines of the electric potential. Deposition of 50 nm particles released at starting points r = i*r_0, i = 0 . . . 10 is uniform on the substrate.

Fierz et al., *Aerosol Sci. Tech.*, 2007

Electrostatic precipitator

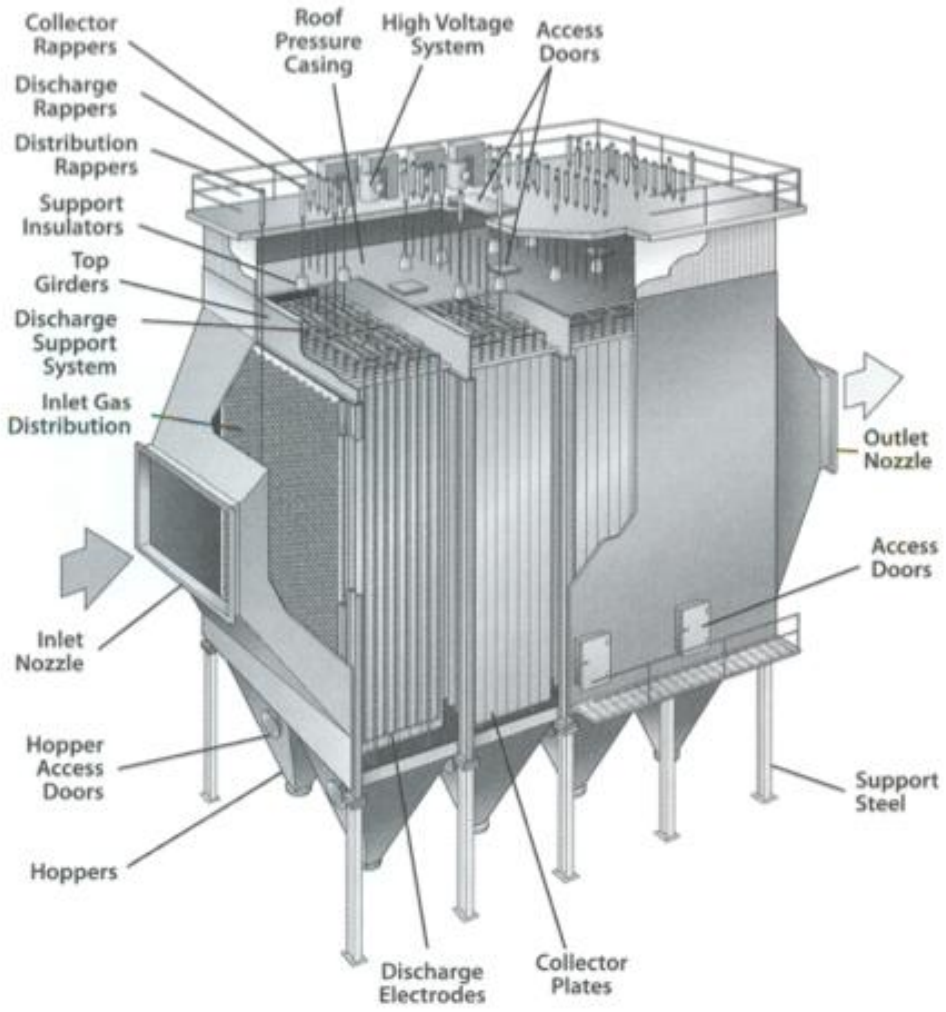

Figure 5.2
Cutaway view of an electrostatic precipitator.
(Courtesy of the Babcock & Wilcox Company, Barberton, OH.)

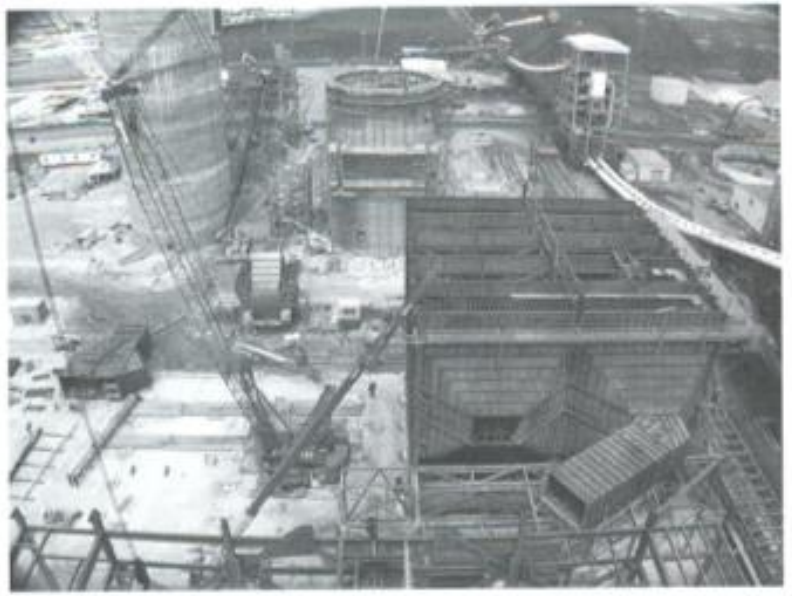

Figure 5.3
An ESP at a coal-fired power plant under construction.
(Courtesy of Siemens Energy, Inc., Orlando, FL.)

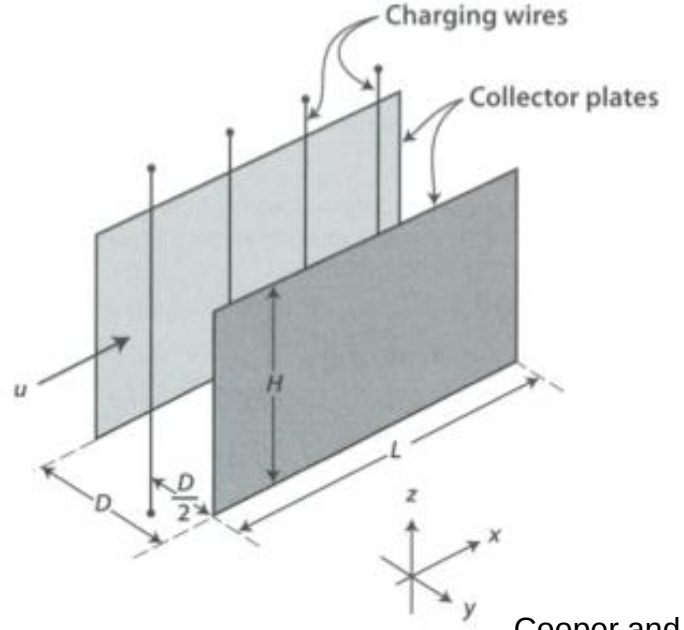

Cooper and Alley, 2006

Figure 5.4
Schematic diagram of airflow between two ESP plates.

measurement of particle size and number
Scanning Mobility Particle Sizer (SMPS)

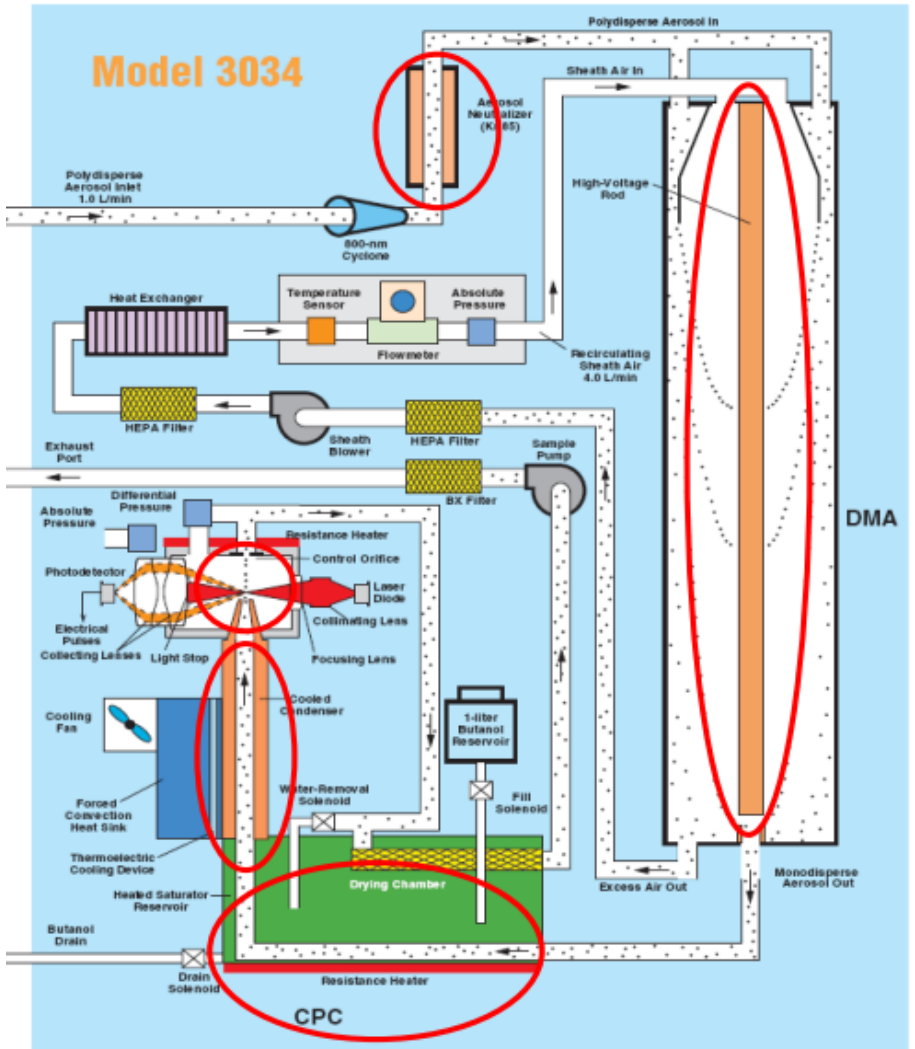

1.Differential Mobility Analyzer (DMA)

Particles are charged and are then separated depending on their size.

Changing the conditions leads to different sizes exiting the DMA.

2. Condensation Particle Counter (CPC)

Selected particles are immersed in a n-butanol flow.

Subsequent cooling leads to enlargement of particles.

Extinction measurement in a laser beam.

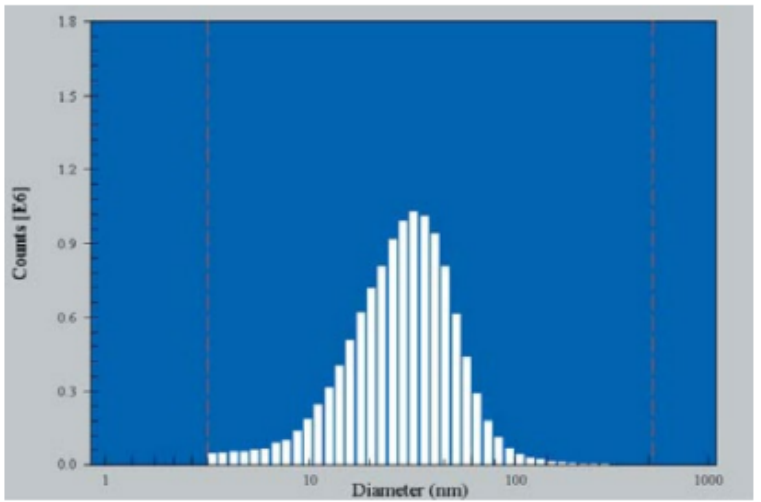

measurement of particle
Scanning Mobility Parti

http://www.tsi.com

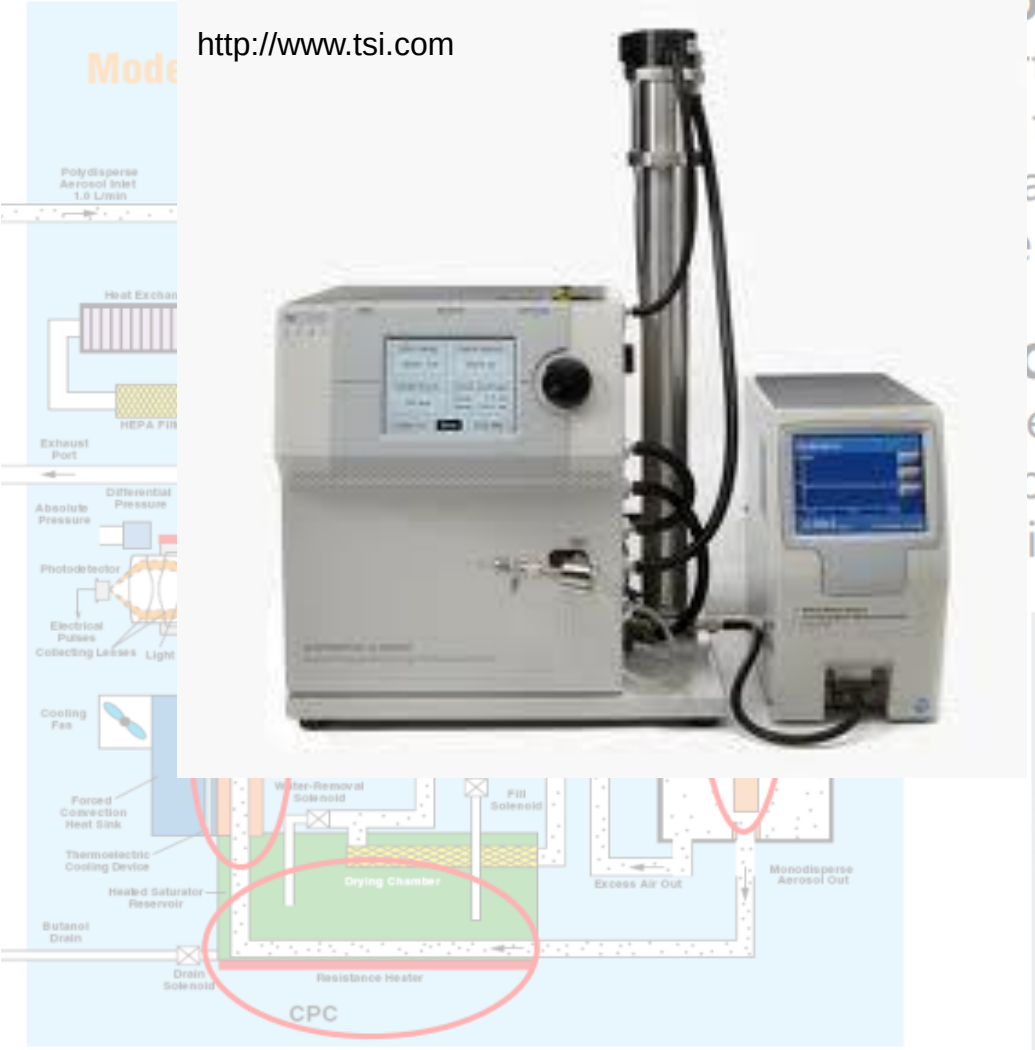

Hinds, 1999

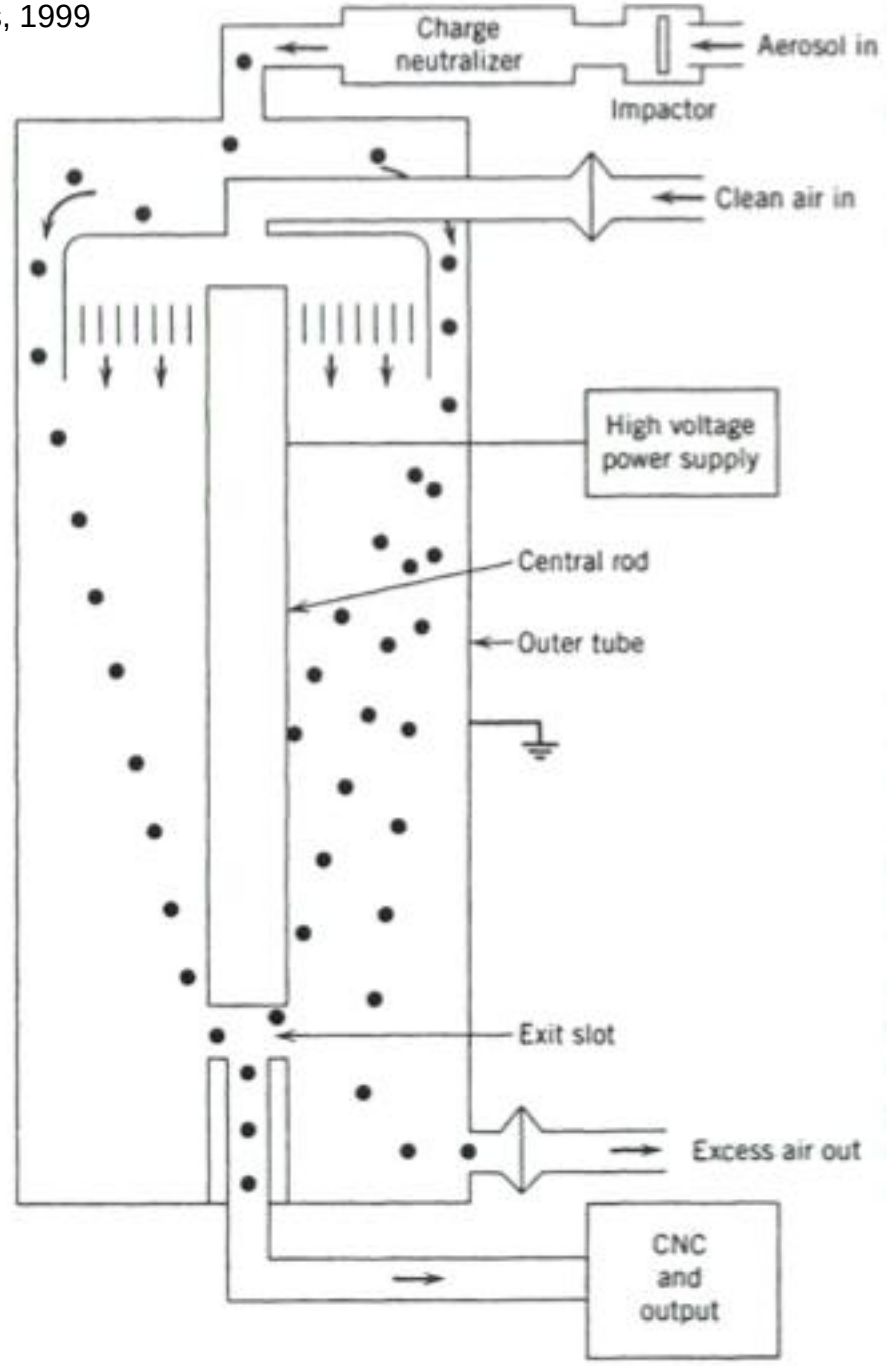

FIGURE 15.12 Schematic diagram of a differential mobility analyzer.

nding
iting
w.
cles.

EPFL 2024

General approach for simulating (individual) particle trajectories (Hinds, 1999)

1. Solve transport equations (e.g., Navier Stokes) for the fluid, with application-specific (e.g., geometric, flow) constraints.
2. Use the velocity fields **u** (and electrostatic fields) generated from their solutions and solve equations of motion for individual particles. This assumes that the following particle-particle interactions are negligible:
   - Coagulation
   - Coulombic (charged)
3. Also neglects gas-particle interactions
4. Repeat for various size particles to generate collection efficiency curve.

Example 1

Adapted from Seinfeld and Pandis (2006)

Let us consider an idealized flow [...] in which an airflow makes an abrupt 90° turn in a corner maintaining the same velocity (Crawford 1976). We would like to determine the trajectory of an aerosol particle originally on the streamline y = 0, which turns at the origin x = 0.

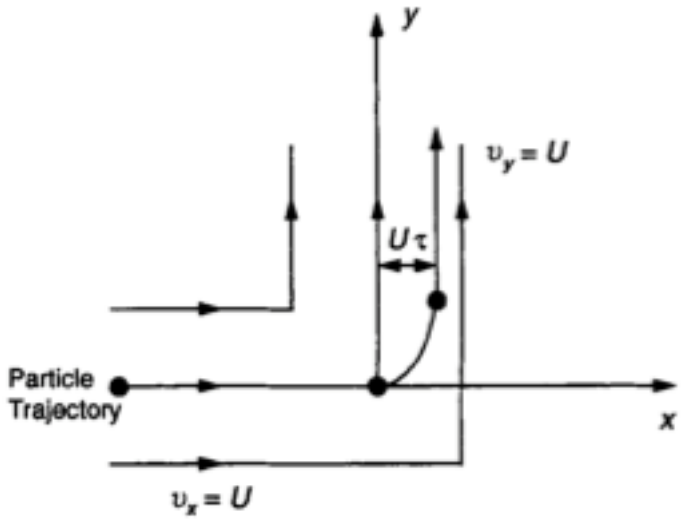

Begin wtih the momentum balance:

$$m_p \frac{d\mathbf{v}}{dt} = \frac{3\pi\mu D_p}{C_c}(\mathbf{u} - \mathbf{v})$$

Let $\tau = m_p C_c/(3\pi\mu D_p)$. Rearranging, we get

$$\tau \frac{d\mathbf{v}}{dt} = \mathbf{u} - \mathbf{v}$$

Vector values in two dimensions using Cartesian coordinate system:

$$\mathbf{v} = (v_x, v_y) = (dx/dt, dy/dt)$$
$$\mathbf{u} = (0, U)$$

So we want to solve

$$\tau \frac{d^2x}{dt^2} + \frac{dx}{dt} = 0$$
$$\tau \frac{d^2y}{dt^2} + \frac{dy}{dt} = U$$

Subject to initial/boundary conditions:

$$x(t=0) = 0$$
$$y(t=0) = 0$$
$$\frac{dx}{dt}(t=0) = U$$
$$\frac{dy}{dt}(t=0) = 0$$

Solution

Note that these are two 2nd-order linear differential equations with constant coefficients:

$$\tau \frac{d^2x}{dt^2} + \frac{dx}{dt} = 0 \qquad \text{homogeneous}$$

$$\tau \frac{d^2y}{dt^2} + \frac{dy}{dt} = U \qquad \text{non-homogeneous}$$

Solution:

$$x(t) = U\tau[1 - \exp(-t/\tau)]$$
$$y(t) = -U\tau[1 - \exp(-t/\tau)] + Ut$$

For $t \gg \tau$,

$$x(t) = U\tau$$
$$y(t) = Ut$$

Larger particles will have a larger relaxation time τ because the numerator scales with $m_p \sim D_p^3$, whereas the denominator scales with D_p. If $U = 20\ \mathrm{m\,s^{-1}}$ and $\rho_p = 2\ \mathrm{g\,cm^{-3}}$

- $x(t \gg \tau) = 0.48$ mm for $D_p = 2\ \mu$m
- $x(t \gg \tau) = 4.83$ mm for $D_p = 20\ \mu$m

Example 2

A 0.2-μm-dimater particle of density 1 $g\,cm^{-3}$ is being carried by an airstream at 1 atm and 298 K in the vertical direction with a velocity of 100 $cm\,s^{-1}$. The particle enters a charging device and aquires a charge of two electrons (the charge of a single electron is 1.6×10^{-19} C) and moves into an electric field of constant potential gradient $E = 1000\ V\,cm^{-1}$ perpendicular to the direction of flow (vertical direction).

1. What is its horizontal and vertical positions after 0.5 seconds? 2 seconds?
2. Calculate positions at the same times for a 50 nm particle.

For this size particle, you can neglect gravity and Brownian motion.

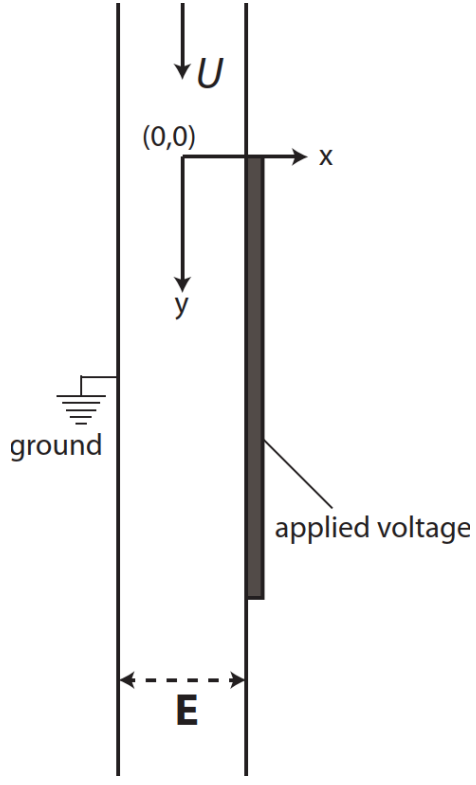

Initial conditions

$$x(t=0) = 0$$
$$y(t=0) = 0$$
$$\frac{dx}{dt}(t=0) = 0$$
$$\frac{dy}{dt}(t=0) = U$$

Equations of motion

$$m_p \frac{d\mathbf{v}}{dt} = \frac{3\pi\mu D_p}{C_c}(\mathbf{u}-\mathbf{v}) + \mathbf{F}_{\text{electrostatic}}$$

$$\mathbf{v} = (v_x, v_y) = (dx/dt, dy/dt)$$
$$\mathbf{u} = (U, 0)$$
$$\mathbf{E} = (0, E)\ .$$

Equations of motion

$$\frac{d^2x}{dt^2} + \frac{1}{\tau}\frac{dx}{dt} = \frac{2qE}{m_p} = \frac{\Phi}{\tau}$$
$$\frac{d^2y}{dt^2} + \frac{1}{\tau}\frac{dy}{dt} = \frac{U}{\tau}$$

Soln to diff eq and application of initial conditions

$$\frac{dx}{dt}(t=0) = -\frac{C_{x,2}}{\tau} + U = U \quad \Rightarrow \quad C_{x,2} = 0$$
$$x(t=0) = C_{x,1} + C_{x,2} = 0 \quad \Rightarrow \quad C_{x,1} = -C_{x,2} = 0$$
$$\frac{dy}{dt}(t=0) = -\frac{C_{y,2}}{\tau} + \Phi = 0 \quad \Rightarrow \quad C_{y,2} = \Phi\tau$$
$$y(t=0) = C_{y,1} + C_{y,2} = 0 \quad \Rightarrow \quad C_{y,1} = -C_{y,2} = -\Phi\tau$$

Final equations

$$x = \Phi\tau\left(e^{-t/\tau} - 1\right) + \Phi t$$
$$y = Ut$$

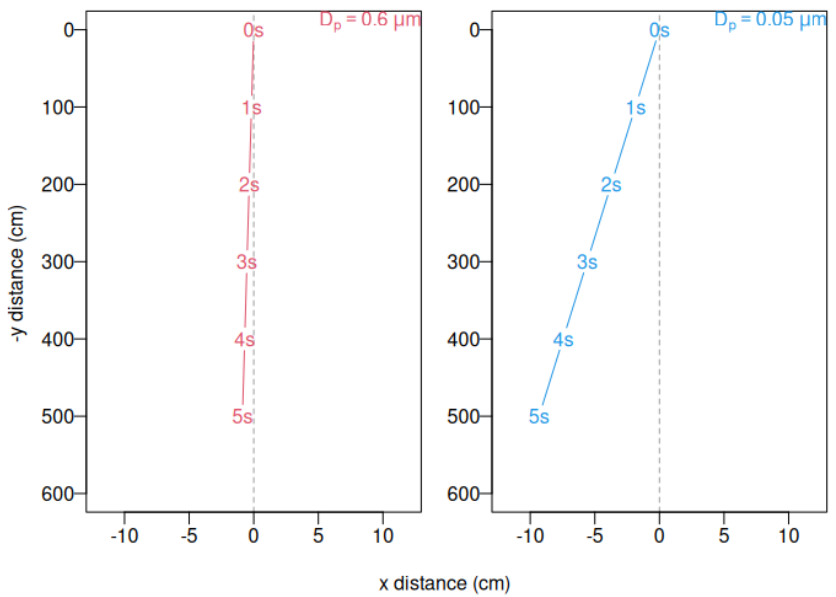

In practice

You often cannot easily solve the equations of motion for the fluid analytically or numerically (e.g., because of complex geometry).

Use CFD/multiphysics simulation package (FLUENT, ANSYS, COMSOL) to generate velocity/electrostatic fields.

Optical measurements

Optical vs gravimetric

Ideal pathway for quantification:

- Light scattering events → particle size distribution
- Integrated volume concentrations → mass concentrations

Light-particle interactions

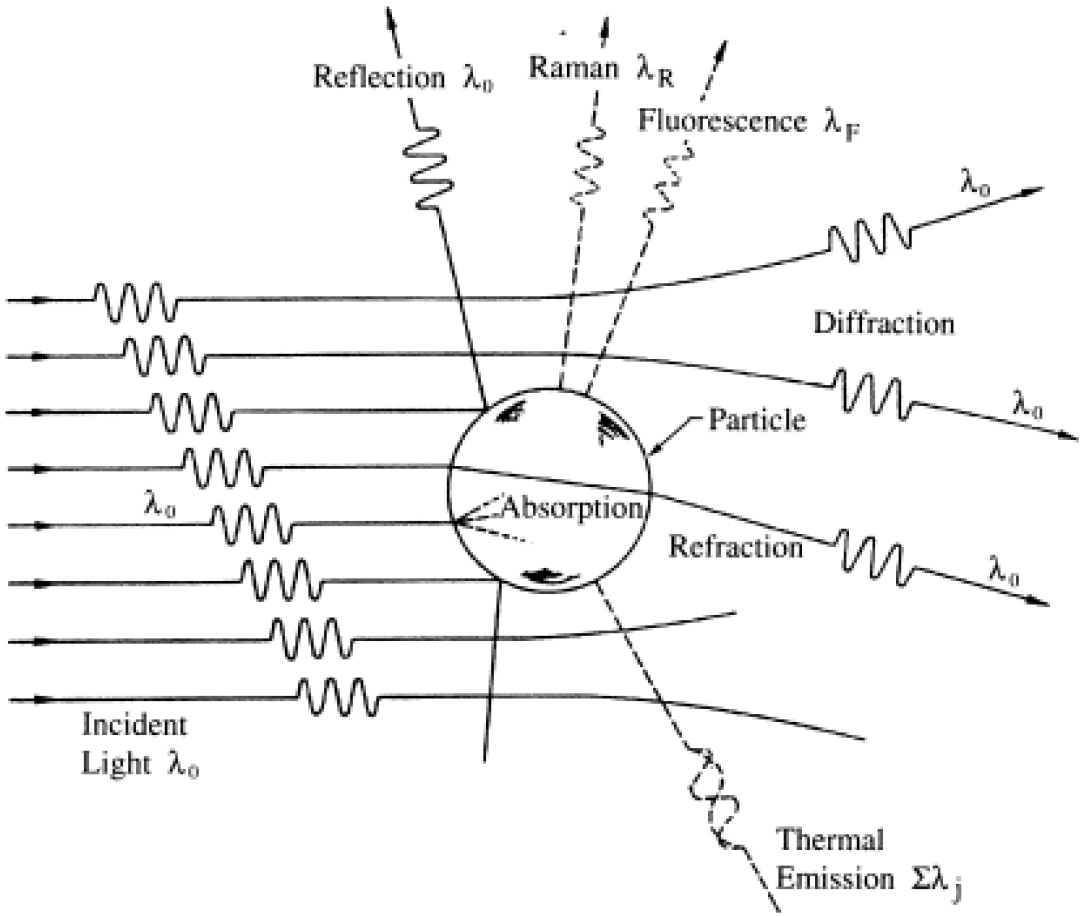

Seinfeld and Pandis, *Atmospheric Chemistry and Physics*, 2016

Optical measurements

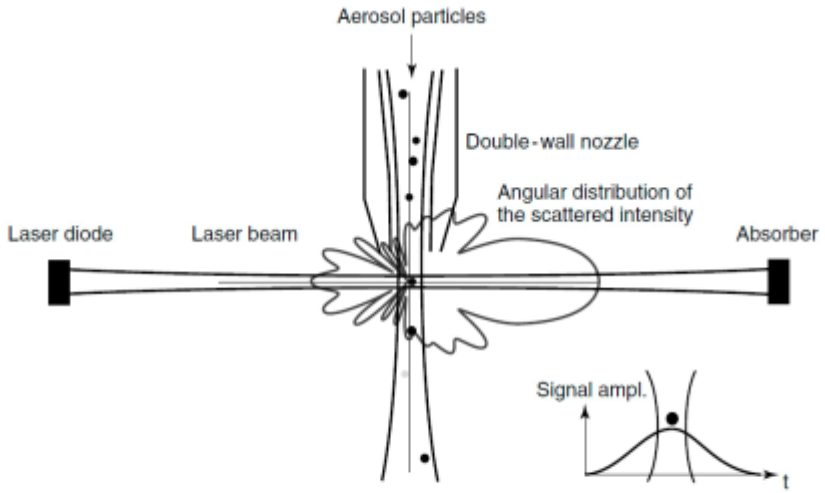

Figure 4. Generic scheme of an OPC: the particle crossing the illumination zone (viewing volume) generates a diffraction pattern at a 360° angle. The corresponding impulse recorded by the photodiode is shown in the inset; the intensity of the signal depends on the particle size, while its width is correlated to the viewing volume (image reprinted with permission of the authors in [59] provided by Wiley—VHC Publisher).

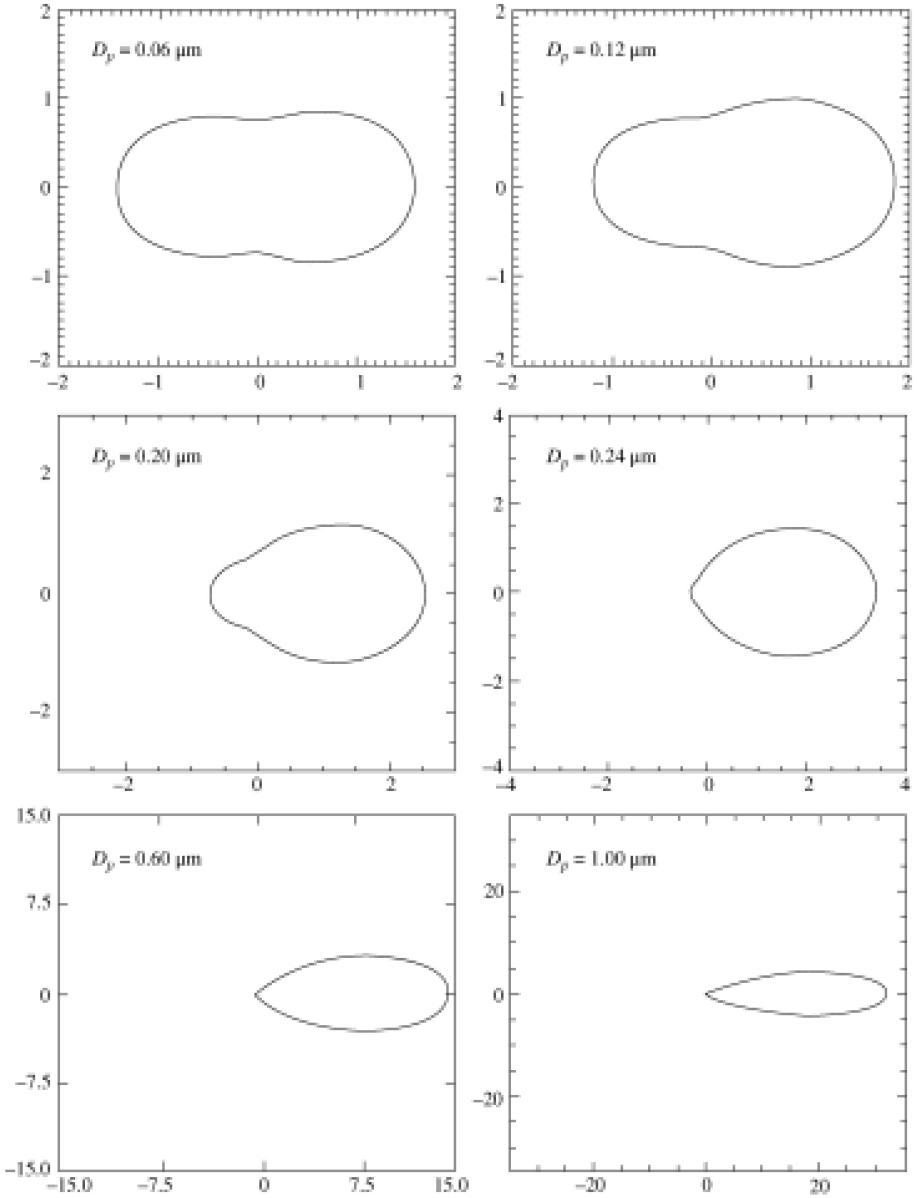

Scattering phase function for incident wavelength of 550 nm

Seinfeld and Pandis, *Atmospheric Chemistry and Physics*, 2016
Alfano et al., *Sensors*, 2020

Particle size and light scattering

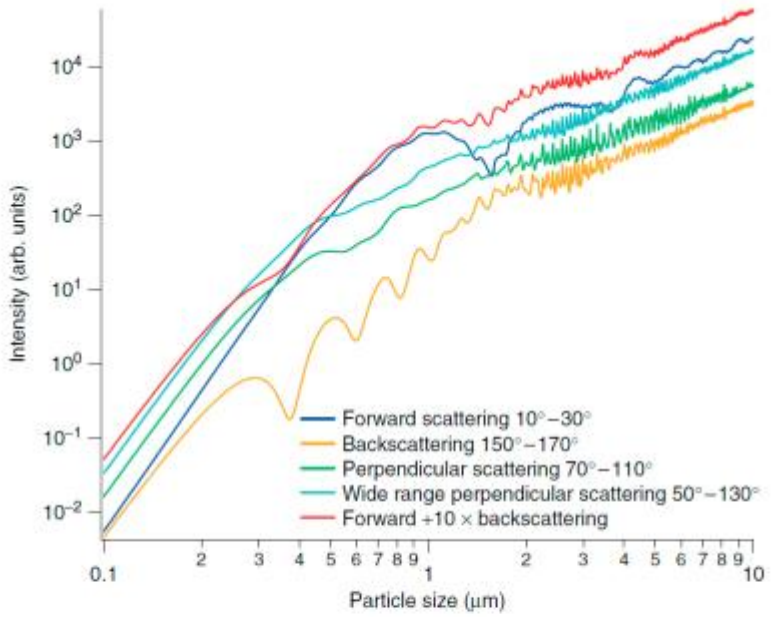

Figure 5. Calculated calibration curves for different scattering angles and integration ranges for polystyrene latex: in the case of forward and back-scattering, the relationship between size and scattering intensity in some size intervals, namely the 0.4–1 μm range for back-scattering and the 1–3 μm range for forward scattering, is not uniform. In the case of perpendicular scattering, shorter oscillations are observed in the range of 2–5 μm; this latter geometry is preferable both for its dimensional distribution and because it has less dependence on the refractive index of the particles (image reprinted with permission of [59] provided by Wiley—VHC Publisher).

Alfano et al., *Sensors*, 2020

Optical Particle Counters

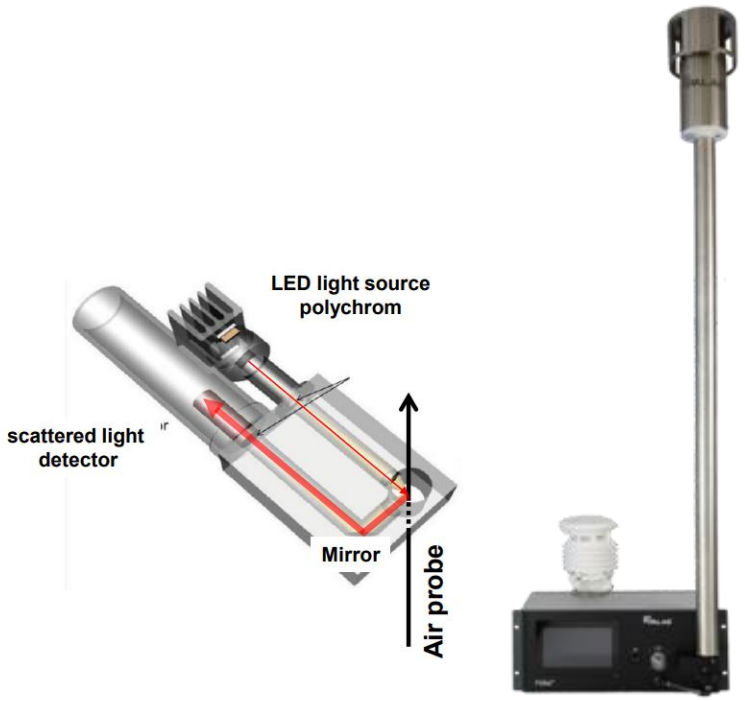

Fidas 2000

Purple Air

Fidas 2000

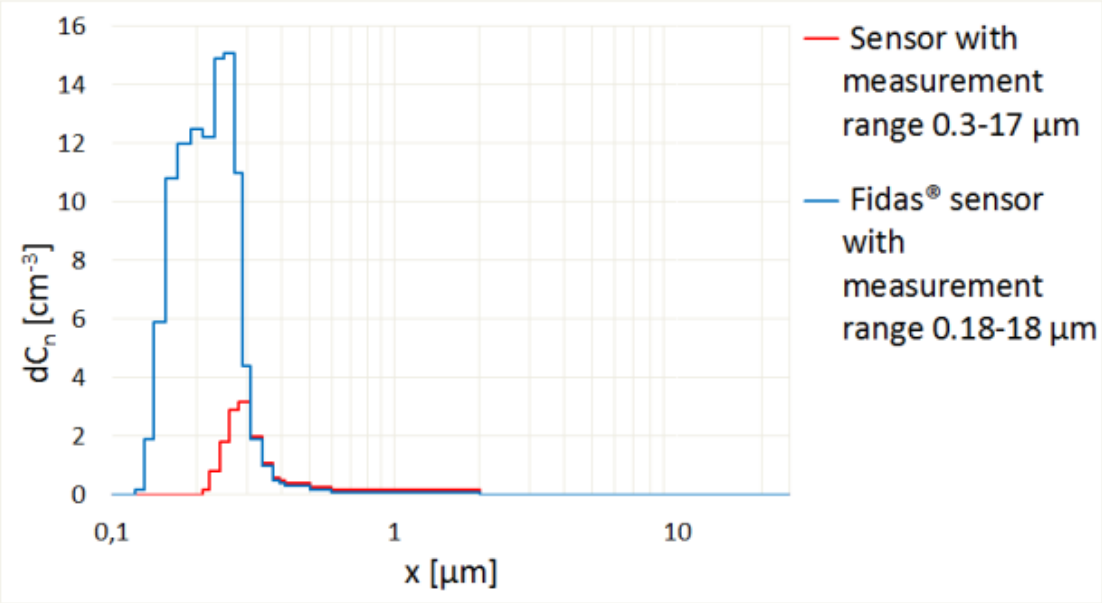

Certified fine dust measurement device Fidas 200, TÜV Rheinland certified, TÜV cer

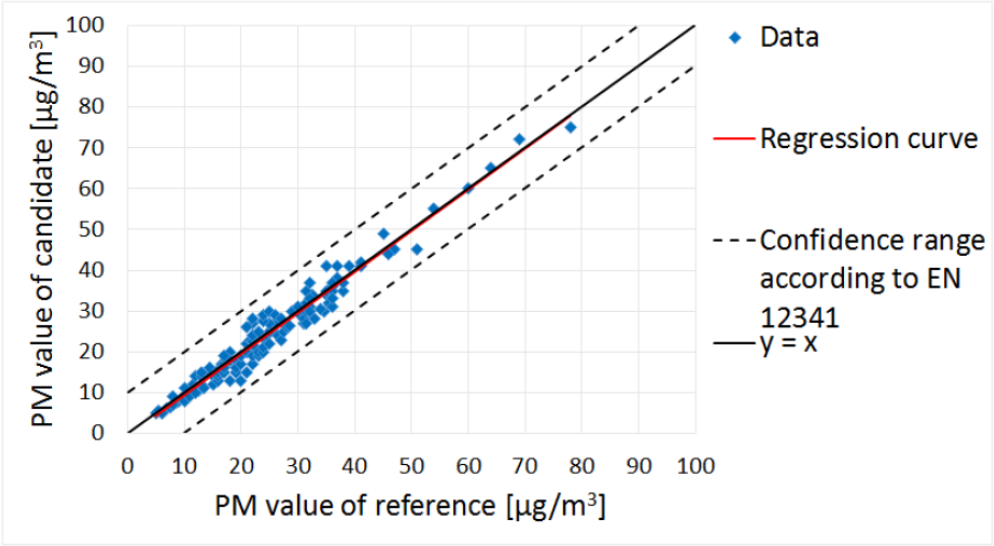

Fig. 3: PM_{10} reference equivalence function of the Fidas® 200 S in comparison with a reference small-filter device during suitability testing from the "Report on supplementary testing of the Fidas® 200 S respectively Fidas® 200 measuring system manufactured by Palas GmbH for the components suspended particulate matter PM_{10} and $PM_{2.5}$, TÜV report no.: 936/21227195/B".

Purple Air - high aspiration efficiency

- Dependent on wind-speed
- Increasingly important for coarse particles
- But small part of quantification error for large particles

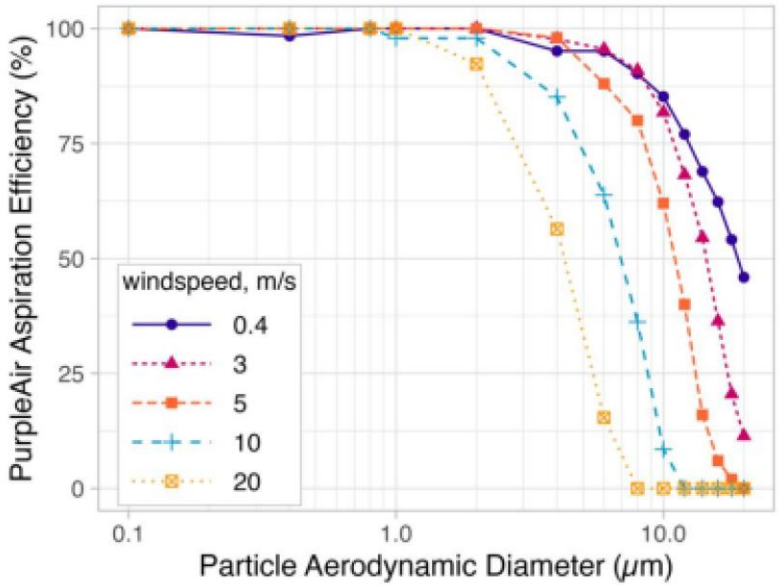

Ouimette et al., *Aerosol Sci. Tech.*, 2023

Purple Air – scattering intensity

- Relationship between scattering between scattering and particle size.
- Approximately unique relationship between particle size and scattering.
- Smallest particles detected by Purple Air sensors ~0.3 µm.

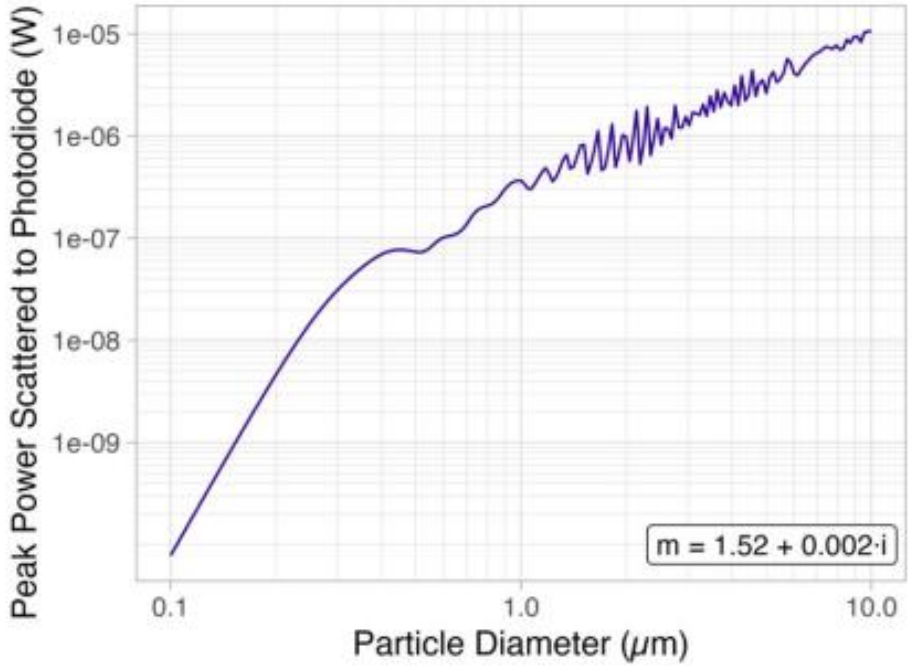

Wavelength ~657 nm

Ouimette et al., *Aerosol Sci. Tech.*, 2023

Purple Air – captured light

- Light from particles are scattered anisotropically.
- Only part of the scattered light is captured by photodiode due to its placement, and also depends on particle position in the laser.

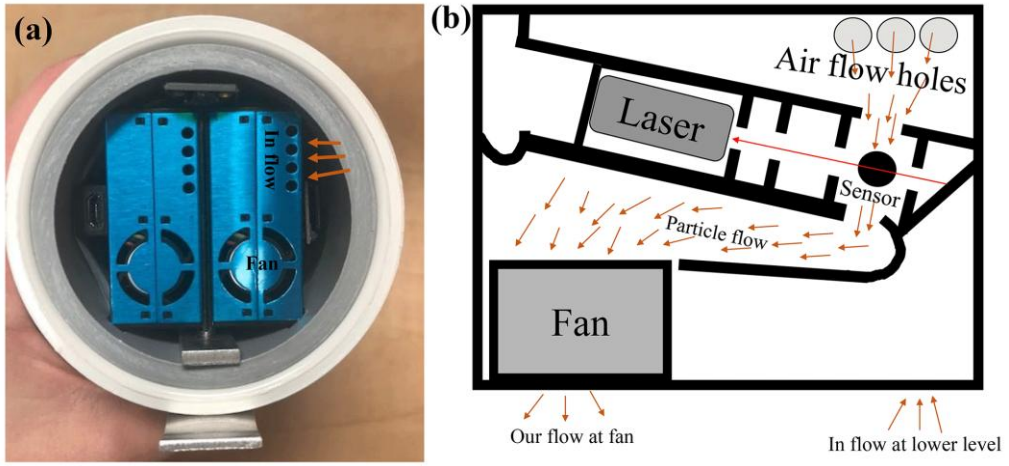

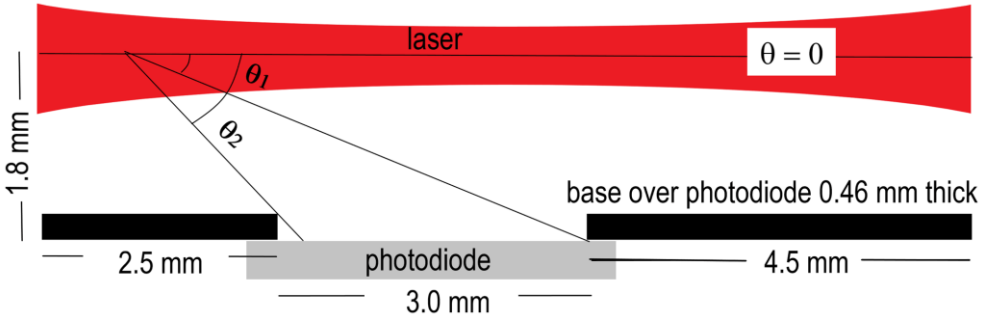

Ardon-Dryer et al., *Atmos. Meas. Tech.*, 2020
Ouimette et al., *Atmos. Meas. Tech.*, 2022

Purple Air particle-laser interactions

Largest source of error in quantification.

“As particle flow is not focused into the core of the laser beam, >99% of particles that flow through the [sensor] miss the laser, and those that intercept the laser usually miss the focal point and are subsequently undersized, resulting in erroneous size distribution data.”

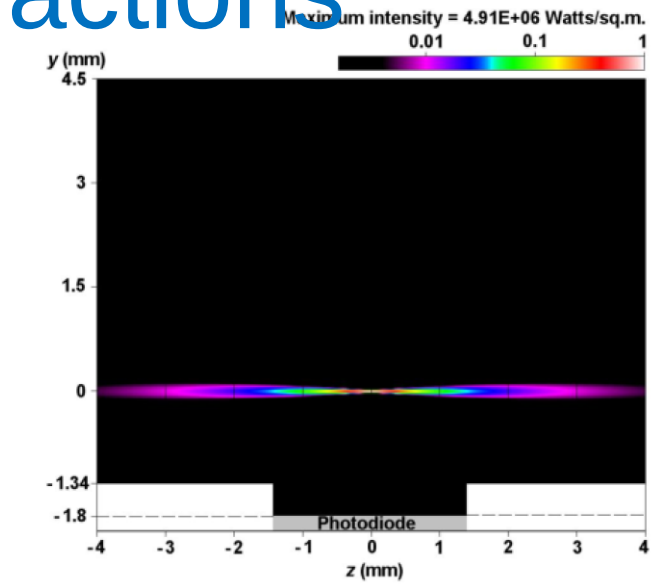

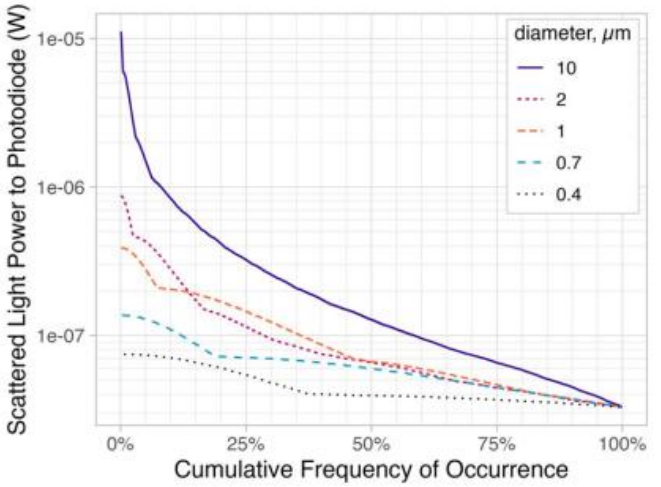

Ouimette et al., *Aerosol Sci. Tech.*, 2023

Comparison of measurement techniques

	Reference (gravimetric)	Purple Air
size selection	size-selective inlet (impactor or cyclone)	no physical device
active sampling	vacuum pump	fan
“capture”	filtration	particle-laser interactions
measurement	gravimetric weight	scattering intensity
time resolution	24 hours	few minutes

Are we measuring the same particles?

- Transmission efficiency
- Sampling/measurement artifacts
- Preconditioning
- Capture or detection

The calibration problem

Atmospheric particles

source: DALL-E

Reference
Gravimetric analysis

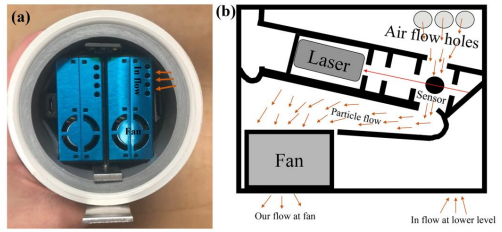

Low cost sensors
Optical

https://metone.com/products/e-frm-dc-reference-method-particulate-sampler/
https://www.sartorius.hr/en/products/laboratory-equipment-and-accessories/laboratory-weighing/laboratory-balances/ultra-micro-laboratory-balances/cubis-ii-ultra-micro-balance/
https://mtlcorp.com/product-category/teflon-pm2-5-filters/
Ardon-Dryer et al., *Atmos. Meas. Tech.*, 2020

Strategies for calibration

Purple Air correction equations

US-wide correction, extended

Low Concentration $PA_{cf\_1} \leq 343\ \mu g\ m^{-3}$ ~176-185 µg m^{-3} as measured by the corrected sensor	$PM_{2.5} = 0.52 \times PA_{cf\_1} - 0.086 \times RH + 5.75$
High Concentration $PA_{cf\_1} > 343\ \mu g\ m^{-3}$ ~207 µg m^{-3} as measured by the corrected sensor	$PM_{2.5} = 0.46 \times PA_{cf\_1} + 3.93 \times 10^{-4} \times PA_{cf\_1}^2 + 2.97$

AirNow Fire and Smoke map

Low Concentration $PA_{cf\_atm} < 50\ \mu g\ m^{-3}$	$PM_{2.5} = 0.52 \times PA_{cf\_atm} - 0.086 \times RH + 5.75$
Mid Concentration $50\ \mu g\ m^{-3} \leq PA_{cf\_atm} < 229$	$PM_{2.5} = 0.786 \times PA_{cf\_atm} - 0.086 \times RH + 5.75$
High Concentration $PA_{cf\_atm} > 229\ \mu g\ m^{-3}$	$PM_{2.5} = 0.69 \times PA_{cf\_atm} + 8.84 \times 10^{-4} \times PA_{cf\_atm}^2 + 2.97$

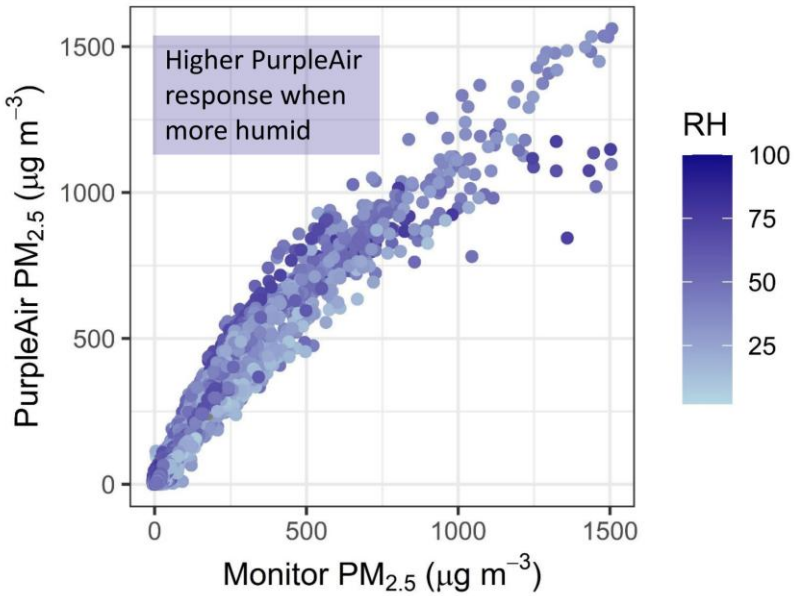

https://cfpub.epa.gov/si/si_public_record_report.cfm?dirEntryId=353088&Lab=CEMM

Calibration models

particle volume

$$PM_{2.5} = \beta_0 + \beta_1 \sum_{D_\mathrm{p}<2.5\mu\mathrm{m}} V_\mathrm{p}$$

(Fidas)

$$PM_{2.5} = f(Response, RH, T_\mathrm{dp}, \ldots)$$

dew point temperature

e.g.,
number concentrations
mass concentrations

illustration of
random forest model

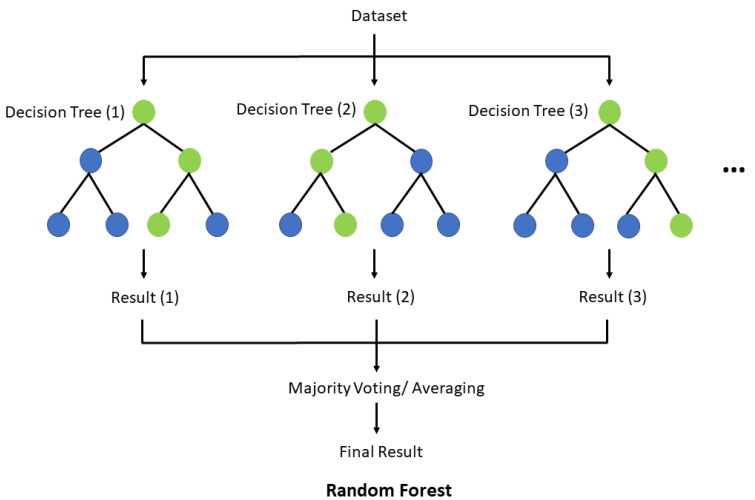

https://de.wikipedia.org/wiki/Random_Forest

Calibration roadmap

Model building phase

- Variable selection
- Sample selection
- Model selection
  - Framework
  - Parameters

Operational phase

- Maintenance
- Flagging data

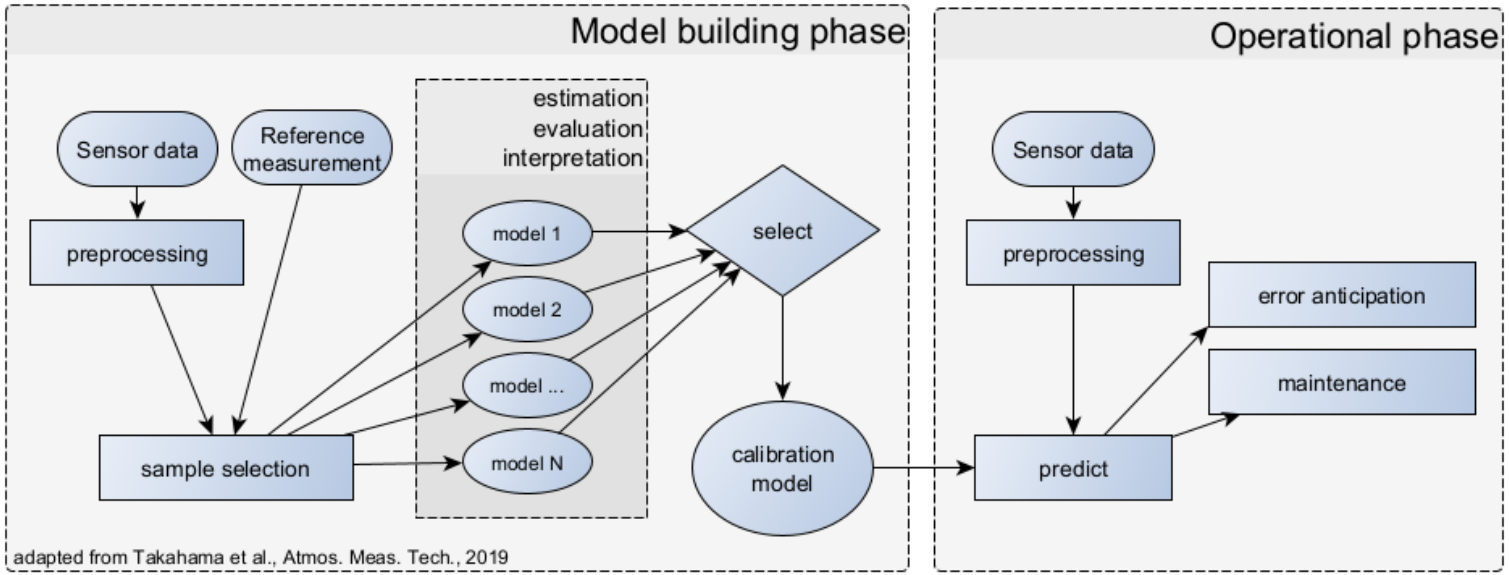

Takahama et al., *Atmos. Meas. Tech.*, 2019

Another optical measurement…

Model 3772

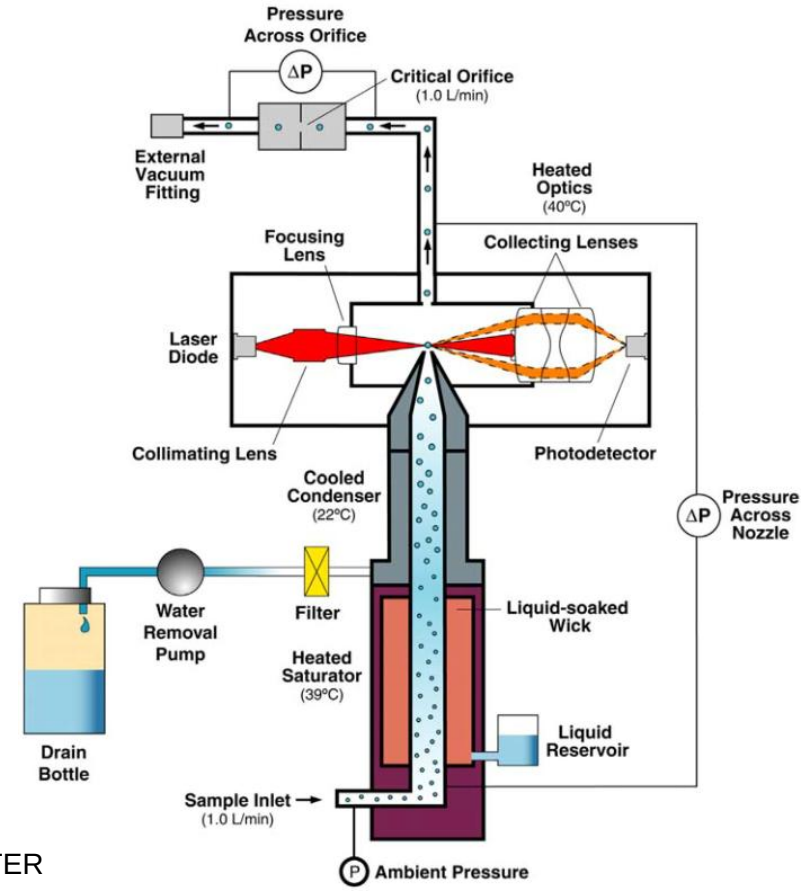

Figure 5-1
Flow Schematic of the Model 3772/3771 CPC

CONDENSATION PARTICLE COUNTER
MODEL 3772/3771
OPERATION AND SERVICE MANUAL

Schweizerische Eidgenossenschaft
Confédération suisse
Confederazione Svizzera
Confederaziun svizra

Federal Office for the Environment FOEN

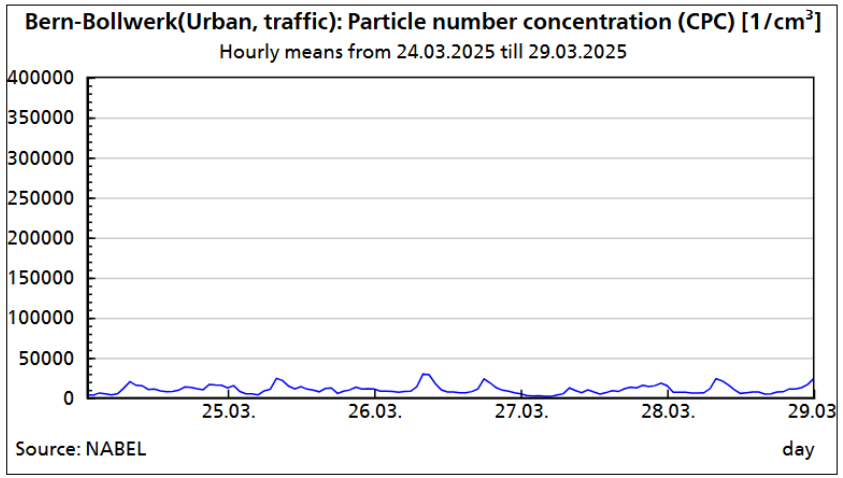

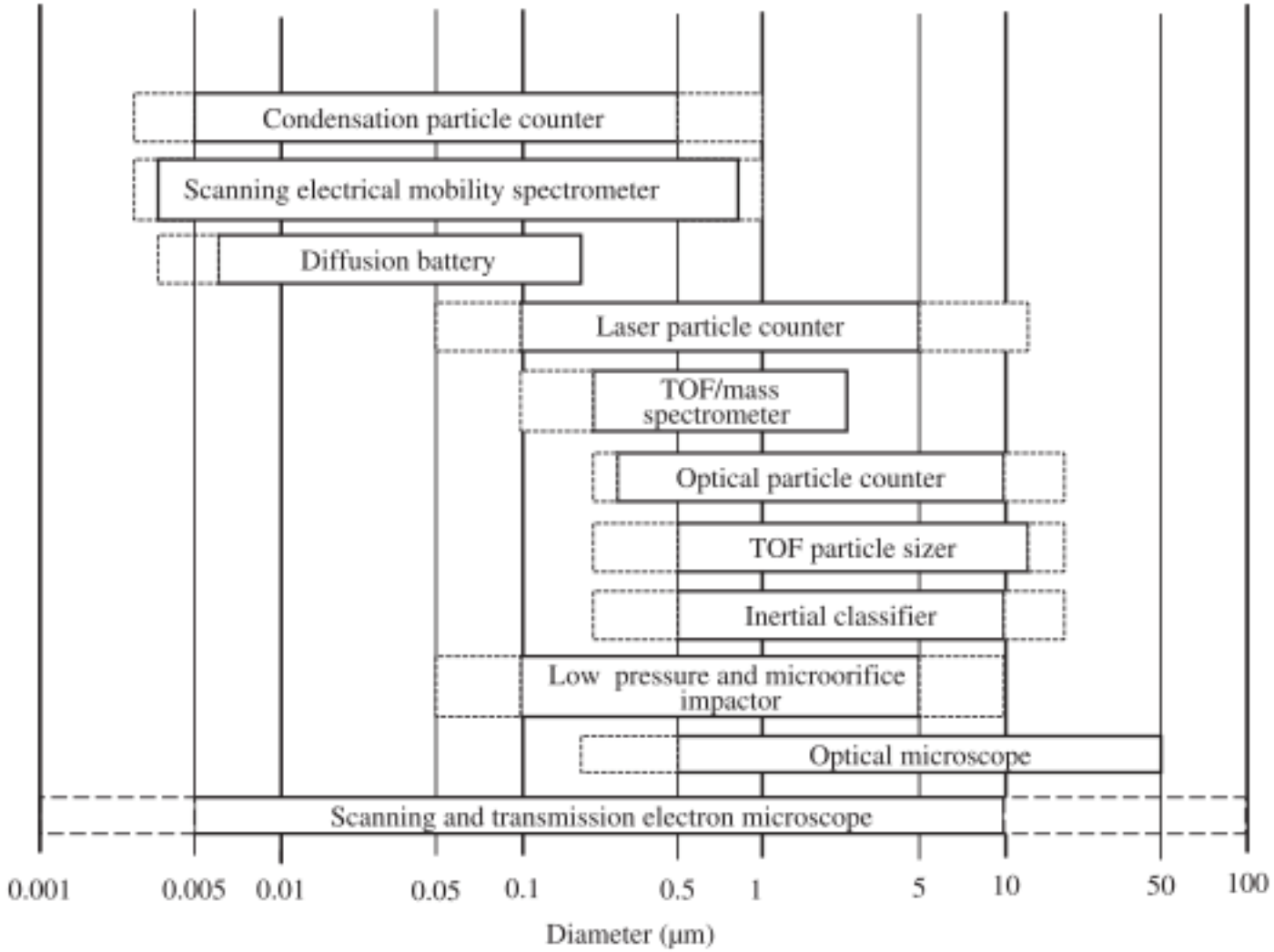

Figure 5-1 Measurement size range of some principal aerosol instruments.

Kulkarni et al., 2011

Summary

- Motion of individual particles can be described by a force balance. (What are the different types of forces?)
- Same mechanistic principles underly sample collection and air pollution control of particulate matter
- What are some challenges for particle collection and measurement?

Further reading

- Barkjohn, K. K., Gantt, B., and Clements, A. L.: Development and application of a United States-wide correction for PM2.5 data collected with the PurpleAir sensor, *Atmospheric Measurement Techniques*, 14, 4617–4637, https://doi.org/10.5194/amt-14-4617-2021, 2021.
- deSouza, P., Kahn, R., Stockman, T., Obermann, W., Crawford, B., Wang, A., Crooks, J., Li, J., and Kinney, P.: Calibrating networks of low-cost air quality sensors, *Atmospheric Measurement Techniques*, 15, 6309–6328, https://doi.org/10.5194/amt-15-6309-2022, 2022.
- Giordano, M. R., Malings, C., Pandis, S. N., Presto, A. A., McNeill, V. F., Westervelt, D. M., Beekmann, M., and Subramanian, R.: From low-cost sensors to high-quality data: A summary of challenges and best practices for effectively calibrating low-cost particulate matter mass sensors, *Journal of Aerosol Science*, 158, 105833, https://doi.org/10.1016/j.jaerosci.2021.105833, 2021.
- Jaffe, D. A., Miller, C., Thompson, K., Finley, B., Nelson, M., Ouimette, J., and Andrews, E.: An evaluation of the U.S. EPA's correction equation for PurpleAir sensor data in smoke, dust, and wintertime urban pollution events, *Atmospheric Measurement Techniques*, 16, 1311–1322, https://doi.org/10.5194/amt-16-1311-2023, 2023.
- Ouimette, J. R., Malm, W. C., Schichtel, B. A., Sheridan, P. J., Andrews, E., Ogren, J. A., and Arnott, W. P.: Evaluating the PurpleAir monitor as an aerosol light scattering instrument, *Atmospheric Measurement Techniques*, 15, 655–676, https://doi.org/10.5194/amt-15-655-2022, 2022.
- Ouimette, J., Arnott, W. P., Laven, P., Whitwell, R., Radhakrishnan, N., Dhaniyala, S., Sandink, M., Tryner, J., and Volckens, J.: Fundamentals of low-cost aerosol sensor design and operation, *Aerosol Science and Technology*, 0, 1–15, https://doi.org/10.1080/02786826.2023.2285935, 2023.
- Zimmerman, N.: Tutorial: Guidelines for implementing low-cost sensor networks for aerosol monitoring, *Journal of Aerosol Science*, 159, 105872, https://doi.org/10.1016/j.jaerosci.2021.105872, 2022.